Astrophysical and laboratory applications of self-alignment

S. A. Kazantsev

Scientific-Research Institute of Physics, A. A. Zhadanov Leningrad State University
Usp. Fiz. Nauk **139**, 621–666 (April 1983)

Self-alignment of excited atoms which is observed in the laboratory and in astrophysical situations is reviewed. It is described classically and in terms of quantum mechanics. Astrophysical manifestations of self-alignment of excited atoms in the solar atmosphere and applications of self-alignment in magnetometry are analyzed. Self-alignment in low-pressure gas-discharge plasmas in the laboratory is described in detail. The cross sections for depolarizing collisions measured by this method are tabulated along with the lifetimes of excited inert gas atoms. These atomic constants can be used in practical magnetometry of the outer solar atmosphere.

PACS numbers: 31.50. + w, 95.30.Es, 96.60. – j, 52.20.Hv

CONTENTS

1. INTRODUCTION

The polarization properties of the optical emission of astrophysical and laboratory sources have been studied extensively in recent years. The polarization of spontaneous emission is determined by an anisotropy of the excitation of atoms, molecules or ions. One mechanism for a preferential linear polarization of the emission from a source is self-alignment, i.e., the appearance of a quadrupole ordering of the angular momenta of excited particles as the result of an anisotropy of internal processes.

A much more frequent situation in many astrophysical entities (interstellar and interplanetary gas clouds, stellar envelopes, quasars, comets, and nebulae) is an external anisotropic excitation of an ensemble of free particles by resonant radiation. The density of matter in these astrophysical entities is very low. Specifically, the number density of particles is so low that there are essentially no collisions between particles. The interaction of an ensemble of free particles with anisotropic fluxes of resonant radiation leads to an alignment of spins, i.e., to an anisotropy of the spatial orientation of the spins of the ground-state particles. Since the relaxation time of ground-state particles is very long, thermodynamically nonequilibrium astrophysical systems of this type are stable and exhibit several important and distinctive properties. These properties have recently been analyzed in detail in connection with the possible use of this phenomenon to extract new information about astrophysical entities. Under laboratory conditions, collisions between particles are extremely effective, and collisional relaxation prevents a deviation from spin equilibrium in the ground state. In several cases, on the other hand, collisional relaxation can be suppressed, and a nonequilibrium ensemble of particles can be deliberately produced. A method for producing such systems was proposed by Kastler and has been described in detail in several reviews and monographs.

Our basic purpose in this review is to examine the self-alignment of the total angular momenta of the particles in the excited state. This self-alignment is observed in laboratory and astrophysical sources of optical radiation. We will also examine the possible applications of this alignment in practical solar astrophysics.

Historically the first observation of partial linear polarization of the emission from an astrophysical source emerged from research on the solar corona. The polarization of the spectral lines which was detected actually resulted from a self-alignment of resonant particles during resonant scattering of radiation from the interior part of the solar atmosphere. It was subsequently suggested that this phenomenon might be exploited for magnetometry. Magnetic fields exist in various astrophysical objects and play important role in the events which occur in them;[1] to a large extent the solar activity is determined by this important characteristic. It is accordingly an important astrophysical problem to develop methods for determining the local magnetic field. The solution of this problem will permit a better understanding of the nature of local and global processes on the sun. In the 1960s and 1970s there was an increase in the number of studies dealing with the problem of determining the magnetic fields in the outer parts of the solar atmosphere by making use of self-

 0038-5670/83/040328-24$01.80

alignment. The reason for the increased interest in this method was that it has definite advantages over other experimental methods.

Self-alignment in an ensemble of excited particles can also be seen in the laboratory, and it is in fact exploited in atomic spectroscopy and plasma physics. The laboratory work on this phenomenon is carried out in the low-temperature plasmas of gas discharges by means of the optomagnetic Hanle effect technique: The polarization characteristics of radiation are observed in the presence of an external magnetic field. The magnetic field disrupts the coherence of the states in the ensemble, thereby changing the polarization characteristics of the radiation. The particular way in which the radiation polarization depends on the magnetic field is determined by the characteristics of the emitting state—its relaxation time and Landé factor—and by the observation conditions. The dependence of the degree of polarization on the magnetic field which is found experimentally is the primary source of information about the atomic constants and particular features of excitation processes in plasmas.

In analyzing the polarization properties of the radiation in astrophysics one generally solves the inverse problem: determining the local characteristics of the objects from the measured distribution of the degree of polarization of the radiation. For measurements of magnetic fields by this method it is necessary to know, in addition to the particular features of the excitation and alignment of the pertinent state, the atomic constants and characteristics of the collisional relaxation in the ensemble of particles, since in certain cases this relaxation may occur and give rise to a further depolarization of the radiation. Collisional depolarization can be taken into account if the cross section for the disruption of alignment is known. This information can be obtained from laboratory studies of self-alignment in the low-temperature plasmas of gas discharges.

In this review we examine several fundamental studies of the spin alignment of free particles under astrophysical conditions which have been carried out in connection with the possibility of determining the characteristics of various objects. We focus on the self-alignment of the total angular momenta of excited particles. We describe it by means of both classical and quantum mechanics. We look at the results of studies of this phenomenon in the emission from the solar atmosphere and also at the results of the use of this effect in magnetometry. We then examine the particular features of self-alignment in a low-temperature plasma and the methods used to observe it experimentally. We discuss the physical results of laboratory research. In addition to describing the general behavior and specific manifestations of self-alignment in gas discharges, we give the lifetimes and the cross sections for depolarizing collisions for several excited levels of inert gas atoms—results obtained by the self-alignment method. Tables in this review compare the results with results obtained by other measurement methods. These atomic constants can be used in the practical magnetometry of the outer part of the solar atmosphere.

2. MANIFESTATIONS OF THE SPIN ALIGNMENT OF FREE PARTICLES IN VARIOUS ASTROPHYSICAL OBJECTS

Research involving the interference of states and the exploitation of this interference to study the properties of atoms and molecules has attracted considerable interest in atomic physics since the 1960s.[3,4,20-22] The conditions for the coherent excitation of an ensemble of particles have been studied, and various physical processes which give rise to such an excitation been examined. It has been pointed out in several places[23,24,26] that in many astrophysical objects the excitation leads to an alignment of the spins of particles. Analysis of the physical conditions in the upper layers of the atmosphere of the sun and other stars, the envelopes of quasars, comets, clouds of interstellar and interplanetary gas, and nebulae[23] has shown that anisotropic fluxes of resonant radiation and particles are by no means rare events. The interaction of these fluxes with the ensemble of particles of interest should lead to an alignment of the angular momenta of the particles in the ground state, and since the densities in these objects are very low, and collisional relaxation is negligible, this alignment may have several important consequences. A detailed examination of self-alignment which has been carried out in a series of papers, discussed below, has shown that alignment can be exploited to obtain new astrophysical information: the local vector magnetic field, the number density of particles in the medium, and the degree of anisotropy of luminous fluxes. From this anisotropy one can calculate the relative positions of various objects. Furthermore, it has been learned that the possibility of alignment under astrophysical conditions must be taken into account in interpreting the results obtained by conventional astrophysical methods.

To describe the alignment of the angular momenta of particles it is convenient to work in the formalism of atomic density in the representation of magnetic quantum numbers.[9-11] Let us assume, as an example, that the spin of the ground state is 1, while that of an excited state is 0. The ground-state density matrix $\sigma_{\mu\mu'}$ (μ and μ' are the projections of the angular momentum onto the quantization axis) generally consists of nine elements. The diagonal elements σ_{11}, σ_{00}, and σ_{-1-1} describe the populations of the states with angular-momentum projections of 1, 0, and −1; the off-diagonal elements of the density matrix describe the phase coupling of these states.

In the interaction of an ensemble of free particles with a beam of unpolarized resonant radiation, the particles are excited and then revert to the ground state. Since a beam of unpolarized radiation may be thought of as an incoherent superposition of right-hand and left-hand circularly polarized waves with identical statistical weights, the ground state of an atom is no longer spherically symmetric because of the conservation of the projection of the angular momentum. States with spin projections of ±1 combine, while the population of the state with the projection of 0 increases and deviates from the equilibrium value. An alignment of the spins

of the particles occurs. Such an ensemble is described by a diagonal density matrix with elements $\sigma_{11} = \sigma_{-1-1} \neq \sigma_{00}$. An important feature of an ensemble of particles with aligned spins is an increase in the transparency of the ensemble for resonant radiation. This effect is important since in applied research much astrophysical information is extracted from measurements of the intensity of transmitted radiation. The effect of a change in the optical density of a medium has been examined in detail by Varshalovich,[23] who calculated the degree of alignment in the case of excitation of a system by a directed flux of unpolarized radiation of low intensity and showed that the optical properties of the medium depend on the alignment. The alignment of the spins of particles may alter the relative intensities of emission and absorption lines corresponding to transitions involving an aligned state. Because of this circumstance, a correct determination of the number density of particles from a growth curve requires the use of the corrections found in Ref. 23.

We will examine a series of studies to illustrate certain new possibilities associated with the alignment of an ensemble of particles in astrophysical objects. A spin alignment is associated with a deviation from equilibrium of the populations of magnetic sublevels. In certain cases the alignment of the ground state of an atom can cause a coherent intensification of radio waves as they are transmitted through a medium. This intensification was studied in Refs. 24–26 for the cases of HI and OH. The alignment of ground-state hydrogen atoms by resonant radiation is an important problem in astrophysics since atomic hydrogen occupies large volumes with a very low density. Under such conditions there are essentially no interactomic collisions, so that in the interaction of free atoms with anisotropic fluxes of ultraviolet radiation in the range 1216–912 Å in the $1S_{1/2}$ ground state the spins of the atoms "line up," and a population inversion forms in the hyperfine levels. In principle there can be a coherent amplification of radio waves at the wavelength 21 cm, and this amplification can occur even if the population inversion is only modest, because of the large dimensions of the amplifying medium.[142] Varshalovich and Komberg[27] have studied interference in quasar envelopes. The alignment in quasar envelopes results from an interaction of particles with directed radiation in the course of resonant scattering or photoionization. In this case the alignment gives rise to a linear polarization in the wings of spectral absorption lines, and it also alters the optical thickness of the system for the various lines in a multiplet, causing deviations of the relative intensities in the multiplet from the calculated values. By studying the polarization and the intensity ratio of the components of a multiplet in the spectrum of a quasar envelope one can thus determine the role played by the anisotropy of the radiative excitation and thus determine the relative distance between the source of the radiation and the absorbing medium. The observation of these features would confirm that the absorption lines are formed in regions close to, rather than far from, the quasar.

Other objects in which alignment has been analyzed are comets. The tails of comets contain many different free atoms and molecules, and conditions quite different from those found in the laboratory prevail: Interatomic collisions are extremely improbable, while the photoexcitation of the radiation from the sun is one of the primary mechanisms for the excitation of particles and gives rise to an alignment in the ground state. Mies[28] has calculated the characteristics of the radiation in the D_1 and D_2 lines of Na^{23} scattered by a cometary atmosphere. Mies found that the anisotropic optical excitation from the sun causes an alignment of the total angular momentum (F) of the $^2S_{1/2}$ ground state, which in turn causes a polarization of the emission from the given part of the comet. The degree of polarization of the D_2 line is 16% for observation at an angle of 90°. This process also changes the populations of the hyperfine sublevels of the ground state, as can be seen in a change in the relative intensities of the D_1 and D_2 lines in the emission spectrum of the comet. The problem has been analyzed in more detail by Varshalovich and Chorny[20] as part of a theoretical study of the possibility of determining the direction of weak magnetic fields, at the level of 10^{-6}–10^{-1} Oe. Analysis of the alignment of the spins of sodium atoms by unpolarized light in a magnetic field showed that a change in the direction of the local field causes, first, a change of the order of 5% in the intensity ratio of the D_1 and D_2 lines and, second, an additional change in the degree of polarization of the D_2 line, and this polarization may change sign under certain conditions. The reason for the dependence of these quantities on the direction of the magnetic field is that under these conditions the alignment axis of the ensemble is symmetric with respect to the direction of the field H. This problem is important because its solution reveals the nature of the magnetic field in the comet: whether it is an intrinsic field or a field of predominantly interplanetary origin.

3. DESCRIPTION OF THE SELF-ALIGNMENT OF AN ENSEMBLE OF EXCITED ATOMS

To describe the self-alignment of the total angular momenta of an ensemble of excited particles it is convenient to begin with the classical model of an atom as a linear oscillator formed by a heavy positive core and an outer electron which is undergoing a forced oscillation under the influence of an incident electromagnetic wave. This model has been used widely since the days of Hanle's work[2] for a graphic interpretation of several optical phenomena associated with the interaction of resonant radiation with an ensemble of particles in an external magnetic field.[3-8] Hanle studied the depolarization of the emission from mercury vapor excited by polarized resonant light in an external magnetic field, and he suggested a simple interpretation for his observations based on the model of a damped electric dipole which is precessing in an external magnetic field. The radiation from a linear harmonic oscillator in the wave zone is represented by spherical electromagnetic waves, and the angular dependence of the radiation intensity is described by

$$J = J_0 \sin^2 \alpha, \tag{1}$$

where α is the angle between the observation direction

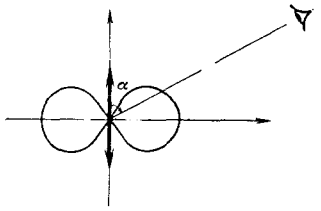

FIG. 1. Spatial diagram of the radiation from an electric dipole.

and the oscillation axis of the oscillator (Fig. 1).

Let us consider an ensemble of free atoms at the origin of coordinates, being bombarded by a beam of linearly polarized light. The light beam is directed parallel to the OX axis, and the polarization vector of the light, $\mathbf{e}_\lambda$, is parallel to the OY axis (Fig. 2). The linear oscillators with axes parallel to $\mathbf{e}_\lambda$ are excited into oscillation, and radiation from them in the OZ direction is linearly polarized with polarization vector parallel to OY. We now impose on this ensemble of atoms an external magnetic field directed along the OZ observation axis, and we orient the axis of the analyzer in the observation channel at an angle β from the OY axis. If the linear oscillator is excited at the time $t=t_0$, then the time evolution of its radiation intensity is described by

$$dJ = J_0 e^{-\Gamma(t-t_0)} \cos^2[\omega(t-t_0)-\beta]; \qquad (2)$$

where $\Gamma = 1/\tau$ is the decay constant of the oscillator, τ is the lifetime of the excited atom, $\omega = \gamma \cdot H$ is the Larmor frequency of the precession, γ is the gyromagnetic ratio, and H is the external magnetic field.

The intensity of the measured polarized radiation from the entire ensemble of atoms is given by the integral

$$J = J_0 \int_{-\infty}^{t} dt_0 e^{-\Gamma(t-t_0)} \cos^2[\omega(t-t_0)-\beta]. \qquad (3)$$

After integrating we find

$$J = \frac{J_0}{2\Gamma}\left[1 + \frac{\cos 2\beta - x \sin 2\beta}{1+x^2}\right] = \frac{J_0}{2\Gamma}\left[1 + \frac{\cos(2\beta + \operatorname{arctg} x)}{\sqrt{1+x^2}}\right], \qquad (4)$$

where $x = 2\omega/\Gamma = 2\gamma H/\Gamma$.

Expression (4) determines the intensity of the polarized resonant radiation from the ensemble of atoms, J, as a function of the external magnetic field H; i.e., it gives the shape of the Hanle-effect signal. It follows from (4) that the measured intensity reaches a maximum when the angle β is $\beta = -(1/2)\operatorname{arctg}(2\omega/\Gamma)$. This means that an external magnetic field rotates the direction of the predominant oscillations of the electric vector of the scattered resonant radiation in the coordinate system selected in the XOY plane, and the rotation angle can be determined by varying the orientation of the axis of the analyzer in the observation channel until the detected intensity is maximized. It can be seen from (4) that the maximum intensity falls off with increasing magnetic field. In a strong field, $\omega\tau \gg 1$, the oscillator will precess at a frequency so high that it performs several rotations in the XOY plane. The radiation detected under these circumstances is depolarized.

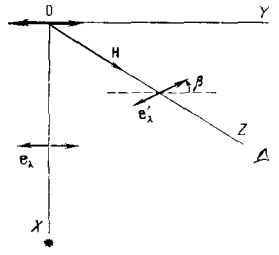

FIG. 2. Coordinate system for describing the Hanle effect.

We now bombard these atoms with a beam of resonant unpolarized light, again along the OX direction. The oscillation of the vector E may be thought of as two mutually orthogonal, uncorrelated oscillations along the OY and OZ axes. These orthogonally polarized waves will excite two incoherent oscillators with oscillation axes parallel to OY and OZ, respectively. Along the OZ observation direction we will again detect linearly polarized emission with a polarization vector parallel to the OY axis, since in this direction the oscillator with oscillation axis parallel to OZ does not radiate (Fig. 1). An external magnetic field applied along the OZ observation axis does not perturb the oscillations of an oscillator with axis parallel to OZ. The change in the polarization characteristics of the radiation detected is due to the precession of an oscillator with an original oscillation axis along OY in the XOY plane, as in the case of a linearly polarized beam of incident light. In the case of excitation by unpolarized light, the qualitative behavior of the polarization of the resonant radiation is thus described by expression (4).

The atomic density matrix is used for a quantum-mechanical description of the alignment of an ensemble of excited particles.[9-11] We assume for simplicity that the angular momentum of the excited state is $J_1 = 1$, while that of the ground state is $J_0 = 0$. In a zero magnetic field the upper state is degenerate in the angular-momentum projection m, which takes on the values -1, 0, 1. If we excite the ensemble of atoms with linearly polarized resonant radiation with a polarization vector $\mathbf{e}_\lambda$ parallel to the OZ axis (Fig. 2), then only the $m=0$ sublevel will be populated in the excited state. The density matrix of the excited state will be diagonal and will consist of only the single element σ_{00}. The populations of the magnetic sublevels of the excited state will exhibit a deviation from equilibrium, and this deviation will be symmetric with respect to the $m=0$ level. In this case the radiation from the ensemble of atoms is linearly polarized. If the polarization of the exciting light is linear, directed along the OY axis, then the structure of the density matrix will be more complex: The sublevels with projections -1 and 1 will be populated in the excited state, and in addition the off-diagonal terms σ_{1-1} and σ_{-11} will arise, reflecting the coherence of the states with the projections of -1 and 1 (Ref. 12). The nonvanishing off-diagonal elements of the density matrix appear because the phase difference between the atomic states with angular-momentum projections will be nonzero when an average is taken over the entire ensemble of radiating atoms. In accordance with the standard terminology, we say that nonvanishing off-diagonal elements of the density matrix represent a coherence. An excitation of an ensemble of par-

ticles which results in the appearance of off-diagonal density-matrix elements is a "coherent excitation." In the case of resonant optical radiation, the coherence of the excitation in the selected coordinate system is achieved by exciting the atoms with radiation which may be represented as a superposition of at least two intrinsic polarizations: σ^+, σ^-, or π. In the case of excitation by natural light along the OX direction (Fig. 2), the excited state is represented by a density matrix in which all the diagonal elements are nonzero ($\sigma_{11} \neq \sigma_{00}$, $\sigma_{-1-1} \neq \sigma_{00}$), and there is a coherence $\sigma_{1-1}, \sigma_{-11}$.

In the density-matrix formalism, the intensity of the radiation detected with a given polarization and in a given direction, $I_{e'_\lambda}$, can be written in the form:[11]

$$I_{e'_\lambda} = c \sum_{mm'} A_{mm'} \sigma_{mm'}, \tag{5}$$

where c is a proportionality constant, and $A_{mm'}$ is the observation matrix, which is expressed in terms of the dipole matrix elements of the transition of interest and which depends on the direction and polarization of the radiation under study, e'_λ.

Expression (5) may be written as the sum of two terms, the first containing only diagonal terms σ_{mm} and the second containing off-diagonal terms $\sigma_{mm'}$ (a coherence). The first term determines the radiation from the ensemble in the absence of phase coupling, i.e., a coherence of states. The second term reflect interference effects in the radiation. It is nonzero if there exist off-diagonal matrix elements of the observation matrix $A_{mm'}$ which correspond to the nonzero values of $\sigma_{mm'}$; i.e., the density matrix of the ensemble contains a coherence, and the observation method can detect it.

The density matrix of the ensemble of atoms can be found by working from the equation of motion derived for it in Ref. 11 under the assumption of weak optical excitation by resonant radiation with a broad spectrum. This assumption holds quite well for the laboratory and astrophysical problems considered in the present review:

$$\dot{\sigma}_{mm'} = -\Gamma_{mm'}\sigma_{mm'} - i\omega_{mm'}\sigma_{mm'} + F_{mm'}, \tag{6}$$

where $\omega_{mm'}$ is the frequency separation of the Zeeman sublevels m and m', $\Gamma_{mm'}$ is the relaxation constant of the density-matrix element $\sigma_{mm'}$, and $F_{mm'}$ is the excitation matrix.

For resonant optical excitation, the matrix $F_{mm'}$, is expressed in terms of the intensity and polarization characteristics of the exciting light and also the matrix elements of the dipole transition in the atom:

$$F_{mm'} = BI_0 \sum_{\mu} \langle \mu | (\mathbf{de}_\lambda) | m \rangle \langle m' | (\mathbf{de}_\lambda) | \mu \rangle \sigma_{\mu\mu}; \tag{7}$$

here B is a proportionality constant, $\sigma_{\mu\mu}$ is the density matrix of the lower level, which is assumed to be diagonal (in the case at hand, $J_0 = 0$, and $\sigma_{\mu\mu'} = \text{const}$), and I_0 is the intensity of the incident light.

Events associated with an interference of states are conveniently described by the formalism of the polarization moments $\rho_q^{(\varkappa)}$, which are the coefficients in the expansion of the atomic density matrix of the excited state, $\sigma_{mm'}$, in components of the irreducible tensor operators of the rotation group, $T_q^{(\varkappa)}$ (Refs. 13 and 14):

$$\sigma_{mm'} = \sum_{\varkappa=0}^{2J_1} \sum_{q=-\varkappa}^{\varkappa} (-1)^q \rho_q^{(\varkappa)} T_{-q}^{(\varkappa)}, \tag{8}$$

$$(T_q^{(\varkappa)})_{mm'} = (-1)^{J_1 - m'} \frac{2\varkappa+1}{2J_1+1} \begin{pmatrix} J_1 & \varkappa & J_1 \\ -m & q & m' \end{pmatrix}, \tag{9}$$

where $\begin{pmatrix} J_1 & \varkappa & J_1 \\ -m & q & m' \end{pmatrix}$ is the Wigner $3j$ number.

The orthogonality condition is

$$\sum_{mm'} (T_q^{(\varkappa)})_{mm'} (T_{q_1}^{(\varkappa_1)})_{mm'} = \frac{2\varkappa+1}{2J_1+1} \delta_{qq_1} \delta_{\varkappa\varkappa_1}, \tag{10}$$

where δ is the Kronecker delta.

Using the orthogonality relation (10), we find the following expression for the polarization moments from (8) and (9):

$$\rho_q^{(\varkappa)} = (-1)^q \frac{2J_1+1}{2\varkappa+1} \sum_{mm'} \sigma_{mm'} (T_{-q}^{(\varkappa)})_{mm'}. \tag{11}$$

The polarization moments $\rho_q^{(\varkappa)}$ have a clear physical meaning. The scalar quantity $\rho_0^{(0)}$ describes the population of the atomic state under study. The three components $\rho_1^{(1)}, \rho_0^{(1)}, \rho_{-1}^{(1)}$ form an orientation vector which is related to the emission of circularly polarized light by the system. The five components $\rho_{\pm 2}^{(2)}, \rho_{\pm 1}^{(2)}, \rho_0^{(2)}$ are an alignment tensor which reflect the quadrupole ordering of the moments in the ensemble of atoms and the emission of linearly polarized light. The component $\rho_0^{(2)}$ of the alignment tensor is called the "longitudinal alignment" and is expressed in terms of the populations of the Zeeman sublevels.

The polarization-moment formalism has proved convenient for problems involving rotations of coordinate systems. The rotations are carried out with Wigner D-matrices.[15,16] The polarization moments with different values of $\varkappa$ do not mix: orientation does not transform into an alignment or vice versa. An equation for the polarization moments of an excited state can be found from (6) through the use of (8)–(11):

$$\dot{\rho}_q^{(\varkappa)} = -\Gamma_\varkappa \rho_q^{(\varkappa)} + iq\omega\rho_q^{(\varkappa)} + F_q^{(\varkappa)}, \tag{12}$$

where $\Gamma_\varkappa$ is the relaxation constant of the polarization moment of rank $\varkappa$. The tensor $F_q^{(\varkappa)}$ describes both the external excitation of the ensemble of particles, which gives rise to the polarization moments, and the mechanisms which operate in the emission sources and cause the self-alignment. This tensor can be derived from (7) for the particular case of the excitation by optical radiation; the result is[14]

$$F_q^{(\varkappa)} = (-1)^{J_1+J_0} B' I_0 \sqrt{2J_1+1} |(J_1 \| d \| J_0)|^2 \begin{Bmatrix} 1 & 1 & \varkappa \\ J_1 & J_1 & J_0 \end{Bmatrix} \Phi_q^{(\varkappa)}; \tag{13}$$

where B' is a proportionality factor, $(J_1 \| d \| J_0)$ is a reduced matrix element, and $\Phi_q^{(\varkappa)}$ is a tensor determined by the characteristics of the exciting light.

For natural light, the components of this tensor, expressed in terms of the angles determining the light propagation direction, $\mathbf{n}(\vartheta, \varphi)$, in a polar coordinate system, are

$$\left.\begin{aligned} \Phi_0^{(0)}(\mathbf{n}) &= -\frac{1}{\sqrt{3}} & \Phi_0^{(2)}(\mathbf{n}) &= -(3\cos^2\vartheta - 1)\frac{1}{2\sqrt{30}}, \\ & & \Phi_1^{(2)}(\mathbf{n}) &= -\sin\vartheta\cos\vartheta e^{i\varphi}\frac{1}{2\sqrt{5}}, \\ \Phi_q^{(1)}(\mathbf{n}) &= 0 & \Phi_2^{(2)}(\mathbf{n}) &= -\sin^2\vartheta e^{2i\varphi}\frac{1}{4\sqrt{5}}. \end{aligned}\right\} \tag{14}$$

In the steady state, we have $\dot{\rho}_q^{(\varkappa)}=0$, and it follows from (12) that the polarization moments can be related in a simple way to the excitation tensor:

$$\rho_q^{(\varkappa)}=F_q^{(\varkappa)}(\Gamma_\varkappa-iq\omega)^{-1}. \quad (15)$$

The intensity of the light emitted with a given polarization e_λ' by the ensemble of atoms in a certain direction can be found if the polarization moments $\rho_q^{(\varkappa)}$ are known. For this purpose we must express the density matrix elements $\sigma_{mm'}$ in the measured intensity $I_{e_\lambda'}$ in terms of the quantities $\rho_q^{(\varkappa)}$ in accordance with (7)–(12). As a result we find

$$I_{e_\lambda'}=(-1)^{J_1+J_0}c'\sum_\varkappa(2\varkappa+1)\begin{Bmatrix}1 & 1 & \varkappa\\ J_1 & J_1 & J_0\end{Bmatrix}\sum_q(-1)^q\rho_q^{(\varkappa)}\Phi_{-q}^{(\varkappa)}(e_\lambda'); \quad (16)$$

where $\Phi_q^{(\varkappa)}(e_\lambda')$ is the tensor determining the observation conditions, and c' is a proportionality factor.

The components of the observation tensor are determined by the characteristics of the radiation being emitted. For observation in unpolarized light, the components of the tensor are described by (14), in which ϑ and φ are angles characterizing the observation direction.

In many laboratory and astrophysical objects the alignment forms as a result of internal excitation processes in an ensemble, e.g., during reabsorption of resonant radiation. In this case we would speak in terms of the self-alignment of an ensemble of particles. In extended sources, if the mean free path of a photon with a frequency corresponding to the center of the spectral line is comparable to the scale dimensions of the source, there is generally an anisotropic optical excitation; the light fluxes incident on the ensemble of atoms from different directions are different. The alignment tensor of such an ensemble can be reduced through rotations of the coordinate system to principal axes determined by the symmetry of the angular distribution of the emission intensity in the source. The process of resonant photoexcitation is universal in nature and can occur both in astrophysical settings and in a broad range of laboratory plasma sources of radiation. A method has been proposed for calculating the polarization moments $\rho_q^{(\varkappa)}$, which determine the characteristics of the scattered radiation and their changes in a magnetic field, for an analysis of this phenomenon in low-pressure gas-discharge plasmas and in solar prominences.[3,17,18] The polarization characteristics of the radiation field produced at a given point by all the emitting particles of the source are described by the polarization tensor $u_q^{(\varkappa)}$:

$$u_q^{(\varkappa)}=\sum_{q_i,\,q_k}(-1)^{q_k}I_{q_iq_k}\begin{pmatrix}1 & 1 & \varkappa\\ q_i & -q_k & q\end{pmatrix}, \quad (17)$$

where $I_{q_iq_k}=\overline{\varepsilon_i(t)\cdot\varepsilon_k^*(t)}$ is the three-dimensional polarization matrix. This matrix is a generalization of the 2×2 polarization matrix which describes a light wave propagating in a certain direction.[19] The quantities $\varepsilon_i(t)$ and $\varepsilon_k(t)$ are the circular components of the electric field vector at the given spatial point, coefficients in the expansion in terms of the circular components $\mathbf{e}_0, \mathbf{e}_1, \mathbf{e}_{-1}$:

$$\mathbf{E}(t)=\varepsilon_0(t)\,\mathbf{e}_0+\varepsilon_1(t)\,\mathbf{e}_1+\varepsilon_{-1}(t)\,\mathbf{e}_{-1}. \quad (18)$$

The tensor components $u_q^{(\varkappa)}$ have a simple physical meaning: $u_0^{(0)}$ is the average intensity of the radiation field $u_{0,\pm1}^{(1)}$ is a measure of the circular polarization, and $u_{0,\pm1,\pm2}^{(2)}$ is a measure of the linear polarization. This representation is convenient for describing an ensemble of particles excited by a resonant radiation field, since in this case the polarization moments can be found from (13) and (15). If the exciting light field is described exclusively by $u_0^{(0)}$ and $u_{0,\pm2}^{(2)}$, which correspond to unpolarized or linearly polarized light, then only the population $\rho_0^{(0)}$ and the alignment tensor $\rho_{0,\pm2}^{(2)}$ form in the excited state. The dependence of the polarization characteristics of the radiation from such an ensemble on the external magnetic field is determined by expression (16).

The self-alignment of an ensemble of excited particles can be observed by studying the polarization characteristics of the radiation: A predominant linear polarization means that this phenomenon is occurring. In addition, information on the state of the ensemble can be found by studying the emission in the presence of an external magnetic field.

4. APPLICATIONS OF SELF-ALIGNMENT IN THE MAGNETOMETRY OF THE OUTER SOLAR ATMOSPHERE

The polarization of the radiation from the outer part of the solar atmosphere has been under continuous study for many years now.[30,31] In several early studies during solar eclipses, the polarization of the radiation from the corona, from deeper parts of the solar atmosphere, and from external formations (prominences) was observed and studied. Analysis of the observations of the continuum and line spectra of the corona yielded explanations for certain features of the radiation from the corona using the model of Thomson scattering of light from the photosphere by free electrons and resonant scattering by free atoms and ions. The first indication of polarization of the spectral lines emitted from the outer part of the solar atmosphere, due to absorption of anisotropic resonance radiation from the inner parts of the atmosphere, was reported in Ref. 32. Ohman[32] predicted polarization of the radiation in the spectral lines of hydrogen and ionized calcium in the radiation from high prominences. A qualitative picture of the polarization state of the radiation from a prominence can be drawn from a classical examination of the alignment process (Section 2). If the ensemble of atoms in a prominence is excited by light from the photosphere, the anisotropy direction of the emitted light will be determined by the OZ axis by virtue of the symmetry of the problem (Fig. 3). As a result, observation in the OY direction will reveal radiation which is partially polarized in the OX direction. The degree of polarization will increase with the height h of the part of the prominence under study, and this corresponds to an increase in the anisotropy of the optical excitation of regions far from the solar limb. The polarization of the radiation in the OY direction will be described in classical terms as the radiation from a linear oscillator whose oscillation axis is parallel to OX, i.e., tangent to the solar limb.

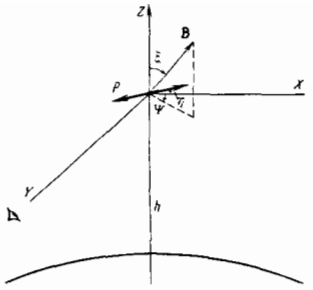

FIG. 3. Coordinate system for describing self-alignment in the solar atmosphere.

Many subsequent experimental observations and studies of the linear polarization of the radiation from prominences were carried out. Fourteen prominences were studied in Refs. 33 and 34 during a solar eclipse, and the polarization of the radiation in the continuum and in the H_α line of hydrogen and the D_2 line of helium was measured. It was found that there is a systematic deviation of the polarization directions of these lines from the tangent to the solar limb. The deviation angles were found to lie in the range 11–30° for H_α and 22–44° for D_3. These experiments spurred some theoretical work,[35,36] in which the polarization of the radiation from an ensemble of atoms in a solar prominence was studied in the classical model of an atomic oscillator. Using a more realistic model of anisotropic photoexcitation, including a limb-darkening effect, Zanstra[35] calculated the degree of polarization of the radiation from a prominence with a small optical density at various points in the prominence for the hydrogen H_α line and the helium D_3 line. It was shown that the scattered light should be polarized tangent to the solar limb. The deviation of the direction of the predominant oscillation of the electric vector in the scattered light wave which was observed in Refs. 33 and 34 was explained by Thiessen[36] on the basis of the Hanle effect, as an effect of the local magnetic field at the observation point on the polarization characteristics. The local magnetic field $B(\xi\psi)$ (Fig. 3) leads to a precession of the oscillator. As a consequence, the polarization plane of the radiation rotates, and there is a decrease in the degree of polarization. The magnitude of the effect depends on not only the magnitude of the vector B but also its spatial orientation, which is specified by the angles ξ and ψ. If the magnetic field is along the OZ axis, it does not change the polarization of the scattered light, since it is directed along the symmetry axis of the optical excitation of the ensemble of atoms. A magnetic field along the OX axis simply reduces the degree of polarization, leaving the direction of the predominant oscillation of the vector **E** in the scattered light wave unchanged. A longitudinal magnetic field along the OY axis will both reduce the degree of polarization and rotate the polarization direction.[17]

Many experimental observations of the polarization of the radiation from prominences in spectral lines were carried out in the 1960s–1970s. The model of anisotropic resonant optical excitation was used to interpret the observations with the goal of determining the local magnetic field. Hyder[37] studied the linear polarization of the radiation from a loop prominence in the bright upper parts of the loop. It was found that the degree of polarization of the radiation in the hydrogen H_α line is 0.8%, and the angles giving the deviation from the tangential direction were 20–25°. According to estimates based on a g_J factor of 1.3 and under the assumption that the prominence had a small optical thickness, these experimental results led to magnetic fields of the order of 45–60 G. Warwick and Hyder[38] studied the polarization of the radiation in the helium D_3 line. They also carried out calculations from the model of an optically thin, collisionless medium for the prominence. The anisotropic photoexcitation of the lower level of the atomic transition of interest, ^3P, by the radiation from the photosphere in the spectral line at 10 830 Å, corresponding to the helium atom transition ^3S–^3P, and the effect of mutliple scattering of phtoons in the medium of the prominence were also taken into account. It was shown that the alignment of the lower level of the transition of interest is inconsequential, while the multiple scattering may strongly affect the polarization. Hyder[39] reconstructed the magnetic field configuration and estimated the field on the basis of polarimeter data. Working from the results of Refs. 33, 34, and 37, Hyder proposed a possible magnetic field configuration in the region of solar prominences. Hyder[39] attributed the cyclic changes observed in the polarization direction of the radiation from prominences to a periodic reversal of the local magnetic field.

The polarization characteristics of the 4227 Å CaI line in the radiation from a quiet prominence were studied in Ref. 40. At an altitude of 15–20 arc seconds the degree of polarization reached 4%, or less than that calculated in the model of anisotropic photoexcitation. The deviation was attributed to two factors in Ref. 40: an additional excitation of the state of interest by isotropic collisions with electrons and the effect of the local magnetic field, whose magnitude was estimated from the Hanle effect to be 25 G.

The possibilities of exploiting the Hanle effect in the radiation from quiet prominences for magnetometry were studied in most detail in a series of studies[17,18,41–44] based on extensive observations, including more than 1000 measurements of the polarization of the radiation from 90 prominences of various types between December 1973 and May 1976. The results of the observations in the helium D_3 line (5876 Å) were summarized in Ref. 41. This line has a rather high radiation intensity, and the results of Ref. 45 indicate that the primary mechanism for the excitation of the D_3 line in prominences is the absorption of resonance radiation from the photosphere. Even for bright prominences in this case, the approximation of an optically thin layer can be used, Substantially simplifying the interpretation of the results of polarimetric measurements. Figure 4 shows histograms of the observations of the degree of polarization and of the rotation of the direction of predominant oscillation of the vector **E** in the scattered light with respect to the tangential direction.[41] The most typical value of the degree of polarization is 1–3.5%, while the rotation angle is ±15°; these quantities vary slightly over the surface of a prominence. A de-

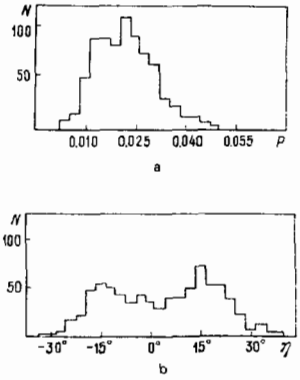

FIG. 4. a—Degree of linear polarization of the helium D_3 line; b—angle of preferential oscillation of the electric vector in the radiation from a quiet prominence according to the data of Ref. 41.

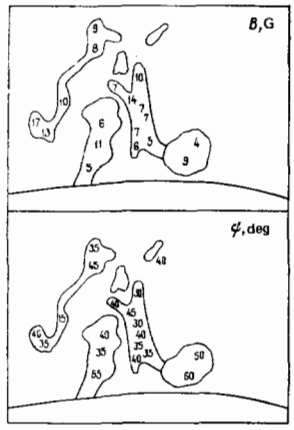

FIG. 5. Map of the magnetic field of a quiet prominence obtained in Ref. 17 through an analysis of the Hanle effect.

tailed study was made of how the degree of polarization, the maximum polarization, the deviation angle, and the intensity of the spectral line depend on the altitude of the region of the quiet prominence under study with respect to the solar limb. Analysis of the results confirms that the magnetic field affects the polarization through the Hanle effect, so that the results can be used to determine the magnetic field. In this series of studies, the local magnetic field B and its spatial orientation, specified by the angles ξ and ψ (Fig. 3), were determined by comparing the observed values of the degree of polarization P, the polarization direction (specified by the angle η; Fig. 4), and the spectral line intensity I_0 with the results of a quantum-mechanical calculation for the Hanle effect for the line of interest in a prominence. This calculation was based on a model of free atoms excited by resonance radiation from the photosphere in the absence of a local magnetic field. The probability for the collisional excitation and depolarization of the line of interest was assumed to be negligible, since collisional processes are important deeper in the solar atmosphere. The polarization tensor of the exciting light field was calculated for each point in the prominence, and then the polarization characteristics of the light scattered in the observation direction were calculated numerically: the emission intensity I_0, the degree of polarization (P) of the helium D_3 line, and the rotation of the predominant-polarization direction (η) as functions of the altitude of the observation point, the density of helium atoms, the electron density and temperature, and the magnetic field vector $B(\xi, \psi)$. These calculations yielded polarization diagrams: families of curves corresponding to the dependence of P/P_{max} and η on the local magnetic field $B(\xi, \psi)$. The calculations were carried out for fields both weaker than[18] 15 G and stronger.[42] In the stronger magnetic fields, the polarization diagrams became multivalued as a result of crossings and anticrossings of the Zeeman sublevels.

This study yielded maps of the magnetic field in quiet prominences according to polarimetric measurements of the helium D_3 line. Figure 5 shows an illustrative magnetic-field map of a prominence observed on 19 December 1974. The measurements of an arbitrarily oriented magnetic field vector can be made more reliable by simultaneously observing the polarization characteristics of the radiation in two helium spectral lines,[46,101] at 5876 and 10 830 Å. In those studies it was assumed that the high optical transparency of the medium would make multiple scattering of photons improbable. On the other hand, an increase in the density of the medium generally leads to absorption of the radiation, and even a few photon reabsorption events can cause a significant additional depolarization of the radiation. This question was taken up theoretically by House and Cohen,[47] who applied the Monte Carlo method to a simplified model of a quiet prominence.

Measurements of the polarization of radiation from the solar atmosphere have long been used for magnetometry.[48-51,44,5] Most solar magnetometers work by means of the Zeeman effect: the splitting of an emission line into orthogonally polarized components in a magnetic field. The Zeeman splitting of a line depends on the nature of the atomic transition and is proportional to the field if the field is sufficiently weak. If the splitting is less than the width of the line, the degree of polarization in different parts of the line contour is measured to determine the magnetic field from the Zeeman effect. Such measurements frequently require a measurement system with a high spectral resolution. Zeeman magnetometry[52] can generally yield reliable values of only the component of the magnetic field which is longitudinal with respect to the line of sight.[53] Attempts to determine the transverse component have not yielded reliable results.[49]

Measurements by means of the Hanle effect do not require a high spectral resolution, since it is the integrated contour of the spectral line which is measured in this method. It is thus possible to improve the spatial resolution of the method and to study fainter spectral lines.[44] This method has one other important advantage in addition to its experimental simplicity: Measurements of two spectral lines make it possible to determine the local magnetic field vector reliably. It should be noted, however, that the present version of the Hanle-effect method is applicable only in cases in which the conditions in the ensemble of atoms under study correspond to a self-alignment by resonance op-

tical emission. On the basis of geometric considerations it is possible to write a description of the anisotropy of the optical radiation and then use additional information on the processes responsible for the formation of the spectral line, on the characteristics of the medium of the object under study, and on the atomic constants to calculate the polarization moments of the upper level of the transition. These moments determine the polarization characteristics of the radiation from the ensemble of particles in the presence of a magnetic field. The local magnetic field can be determined by comparing the measured and calculated values.

An important feature of a Hanle-effect magnetometer is its sensitivity to the strength of the magnetic field being measured. The sensitivity is greatest under the condition $1 \leq \omega\tau^{(2)} \leq 10$, i.e., when the Larmor precession frequency of the atomic oscillator in the magnetic field, ω, is approximately equal to the corresponding relaxation constant $1/\tau^{(2)}$. In this case (Section 2), the radiation may contain a noticeable magnetic-field-induced rotation of the polarization plane, and the degree of polarization may be reduced. Under the condition $\omega\tau^{(2)} \gg 1$ the degree of polarization drops to a minimum value independent of the magnetic field. If $\omega\tau^{(2)} \ll 1$, the magnetic field does not cause any significant change in the direction or degree of polarization of the radiation [see (4)]. Consequently, the lifetimes of the excited atoms must be of the order of 10^{-7} s for measurements of magnetic fields of the order of a gauss. Spectral lines suitable for Hanle-method measurements were selected in Refs. 5 and 44, with allowance for the typical magnetic fields in the various parts of the solar atmosphere. For the corona these fields are generally 10^{-4}–10^{-5} G, so that the method can be implemented if the relaxation constant of the upper level of the transition of interest lies in the range $10 \leq 1/\tau^{(2)} \leq 5000$ s^{-1}. In the solar corona one observes forbidden lines corresponding to magnetic-dipole transitions in multiply charged iron and calcium ions. A detailed analysis of the conditions for the excitation of the lines 5303 Å Fe XIV and 10747 Å Fe XIII carried out in Refs. 54 and 5 showed that the anisotropy of the excitation of these lines and thus the nature of the polarization of the scattered light are determined to a large extent by photoexcitation of the photosphere. Charvin[54] has carried out detailed calculations of the polarization of the radiation in the green line 5303 Å Fe XIV for several models of the corona and for several simple magnetic-field configurations; radiative and collisional excitation and the local magnetic field were taken into account. Expressions were derived for an upper limit on the degree of polarization as a function of the distance from the edge of the disk, and it was shown that under favorable conditions measurements of the polarization could furnish in the first place information on the direction of the projection of the local magnetic field onto the plane perpendicular to the observation line and, secondly, the electron density in the plasma. These measurements become more reliable when simultaneous use is made of several spectral lines.[55] The possibilities of magnetometry of the solar corona on the basis of polarimeter measurements were also examined in a number of studies[55-60] of the polarization of the radiation from an ensemble of particles in the case of anisotropic excitation by resonance radiation from the photosphere. In a model with a corona of nonuniform temperature and density, with an arbitrary spatial distribution of the magnetic field, the degree of linear polarization and the rotation of the polarization plane were calculated with allowance for integration along the observation line. The results apply to both electric and magnetic-dipole transitions.

Hyder's analysis[61] of the polarization studies of solar corona lines was based on Hyder's own measurements and measurements by other workers. The measurements were made for several spectral lines of multiply charged ions, Fe X–Fe XV and Ca XV. Under the assumption of an optical mechanism for the alignment, the the degree of polarization of the radiation from an ensemble of particles was calculated as a function of the distance to the solar surface. The resulting theoretical values were compared with measurements for lines with known g-factors and with known lifetimes for the upper levels of the transitions. It was found as a result that the range of magnetic fields in the solar corona is $5 \cdot 10^{-6} \leq B \leq 5 \cdot 10^{-6}$G. In a detailed study of the green line 5303 Å XIV and the red line 6374 Å Fe XV of the solar corona.[62] it was found that the degree of polarization of the green line varies over the range 2–25% for $1.0 \leq R/R_\odot \leq 1.5$, while that for the red line is at the level of $2 \pm 3.5\%$, in agreement with the calculations of Refs. 54 and 61. The polarization of the Fe XV and Fe XIII corona lines was studied theoretically in a number of papers,[63-65] where the role played by depolarizing collisions of protons was taken into account along with alignment in the photoexcitation of ions. The polarization characteristics of the green line of Fe XIV were analyzed in Ref. 64 under the condition $\omega\tau^{(2)} \gg 1$, i.e., in the absence of a Zeeman coherence in the system. In this case the ensemble of particles is characterized exclusively by the population and longitudinal alignment, while the radiation from the ensemble is characterized by the intensity and degree of linear polarization, which depend on the orientation of the magnetic field, the temperature, the electron and ion densities, the degree of ionization, and other parameters. The theoretical investigation of the polarization of the radiation in the ultraviolet lines 1394 Å Si IV and 977 Å Ca III in various parts of the chromosphere and the corona was carried out[66,67] in a model of coherent optical excitation in the absence of a magnetic field. The effect of a weak magnetic field and of collisions in an optically dense medium on the polarization of the emission of these lines was studied in Ref. 68.

These studies show that self-alignment in the ensemble of free atoms or ions in the outer part of the solar atmosphere is the basis for a method for measuring the local magnetic field. A quantitative analysis of the magnetic field in these regions has been carried out.[5,44]

5. SELF-ALIGNMENT OF ATOMS IN THE PLASMA OF A GAS DISCHARGE

The self-alignment of excited particles was observed in the laboratory well after it was observed in astro-

physics. The particular object in which self-alignment was detected, and studied in detail, was the low-temperature plasma of a gas discharge. The first studies in this direction were reported in Refs. 69–71. In Ref. 69, interference effects were observed in the emission from the plasma of an rf E-type discharge at low pressures. These effects were attributed to an anisotropy of the electron velocity distribution. The self-alignment in the plasma of a positive column which was described in Refs. 70 and 71 resulted from self-absorption of the radiation in the source, i.e., from the same mechanism as in the solar atmosphere.

The alignment of excited atoms in the course of self-absorption of radiation in a source has been studied experimentally and theoretically in a large number of studies. A distinguishing feature of the laboratory experiments in this case stems from the possibility of arranging an optically dense and transparent medium. For a medium with a low optical density, one can treat the interaction of atoms with anisotropic radiation fluxes in the source. The ensemble of excited atoms formed during the absorption of resonance radiation is described by polarization moments consisting of the population $\rho_0^{(0)}$ and the alignment tensor $\rho_0^{(2)}$; the principal axes of the alignment tensor are directed parallel to the symmetry axes of the particular apparatus. Radiation from such an ensemble may be described as radiation from three dipoles of equal intensity which are orthogonal and phase-uncorrelated.[3] The symmetry of the distribution of such dipoles in the source is determined by the shape of the source. In a cylindrical discharge tube, the distribution of these dipoles is cylindrical, while in a spherical volume it is radial. An alignment whose properties are determined by the spatial distribution of the emitting and absorbing particles is conveniently called a "macroscopic" alignment. In astrophysical situations one is generally dealing with a medium of substantial optical transparency, and a predominantly macroscopic alignment will presumably form during the absorption of radiation.

At high optical densities of the medium, an alignment of a different type, "latent," can form.[72] The concept of a latent alignment is related to the interaction of an ensemble of atoms having a specified velocity vector v with spatially isotropic radiation having a finite spectral width (Fig. 6). The alignment of this subensemble is determined by the circumstance that, with a finite spectral width of the irradiating line, the probability for optical excitation is different along different directions with respect to the velocity v. For a Doppler-broadened line the intensity of the exciting light in the direction perpendicular to v is determined by the intensity of the corresponding central frequency of the Doppler contour. Excitation in the direction specified by the vector n corresponds to a harmonic of the Doppler contour at the frequency

$$\nu = \nu_0\left(1+\frac{\mathbf{vn}}{c}\right), \tag{19}$$

where ν_0 is the central frequency of the contour.

Anisotropic excitation of this ensemble of atoms gives rise to alignment. The alignment axis is related to the

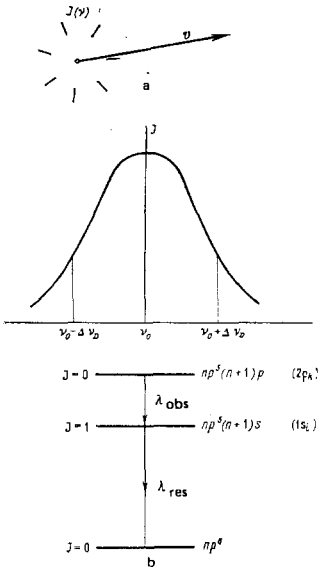

FIG. 6. a—Diagram illustrating the mechanism for latent alignment; b—scheme of transitions in inert gas atoms for observing self-alignment in plasmas.

direction of v. Because of the random distribution of the velocities of the atoms, however, no macroscopic alignment forms in the ensemble. This is the reason for the name "latent" alignment. Chaĭka[73] has analyzed the radiation from an ensemble of atoms in a state of latent alignment. It was shown that, if the velocity of an atom is assumed to remain constant upon the absorption of a photon, the latent alignment gives rise to a change in the emission line contour, which in turn causes the state population $\rho_0^{(0)}$ to become dependent on its alignment. This effect causes the population to become dependent on the external magnetic field. The dependence of the population N on the magnetic field was calculated in Ref. 74 under the assumption that there is no macroscopic anisotropy of the radiation and under the assumption that the line contour which is formed after each successive reemission event remains constant over the entire volume. These calculations led to

$$N = N_0 + N_1 \cdot \left(\frac{1}{1+4\frac{\omega^2}{\Gamma_2^2}} + \frac{1}{1+\frac{\omega^2}{\Gamma_2^2}}\right). \tag{20}$$

The self-alignment of atoms in an ensemble with radiation capture was also studies in Refs. 75 and 76, where a more general model incorporating the change in the velocity distribution of the excited atoms and a redistribution among the Zeeman levels of the excited state was studied. The study was based on an analysis of an equation for the atomic density matrix $\sigma_{mm'}$. This equation can be written in the following general form, where relaxation and radiation capture are taken into account:

$$\frac{d\sigma_{mm'}}{dt} = -\Gamma\cdot\sigma_{mm'} + \Gamma(\hat{L}\hat{\sigma})_{mm'}, \tag{21}$$

where Γ is the reciprocal of the lifetime of the state, and $\hat{L}$ is the radiation capture operator.

In the strong-capture approximation, in which the mean free path of a photon at the center of the line is much shorter than the characteristic dimension of the apparatus, it was shown that alignment with a Maxwel-

lian velocity distribution arises in the ensemble of excited atoms. This alignment is seen in the radiation integrated over the spectrum. This type of alignment corresponds to the macroscopic alignment introduced above. In addition, there are anisotropic distributions of the atoms in the velocity and in the projection of the angular momentum, which are characteristics of the latent alignment. The latent alignment is manifested in an investigation of the spectral distribution of the line polarization, and it has different effects on different parts of the line contour.

Experimentally, different types of alignment have been observed in the plasmas of the positive column of dc discharges in inert gases. At pressures of the order of a few torr the mean free path of a photon at the center of the line for the resonance radiation corresponding to transitions $np^6-np^5\,(n+1)s$ is much smaller than the characteristic dimension of the apparatus: The radiation in the plasma is isotropic. For transitions between excited states belonging to the configurations $np^5(n+1)s$ $np^5(n+1)s-np^5(n+1)p$, under the same conditions, the resonance optical radiation in the plasma has a significant spatial anisotropy. Consequently, in the course of self-absorption in the source, it is basically a latent alignment which forms on the resonance levels, while on the levels of the $np^5(n+1)p$ configuration ($2p_i$ in the Paschen notation) the alignment is basically macroscopic.

Macroscopic alignment in a plasma at these pressures was observed in several studies[77-84] in lines emitted in $1s_k-2p_i$ transitions. Since the resonance radiation from inert gases corresponding to transitions to the ground state of the atoms lies in the far-ultraviolet region, the latent alignment of resonance levels is observed in a stepped process. The changes in the populations of the levels of the $np^5(n+1)p$ configuration with the total angular momentum $J=0$ have been studied in a weak magnetic field.[70] Experimental proof was reported in Ref. 85 of a relationship between the experimental signals of this type and a magnetic-field-disruption of the latent alignment of the resonance levels of inert gases.

In addition to radiation reabsorption, another mechanism operates in a discharge plasma which can cause an alignment of excited atoms. This mechanism involves electron-impact excitation in the case of anisotropic electron velocity distribution. Electron-impact alignment has been observed in rf discharges in several levels of helium[69] and in a group of highly excited levels of inert gas atoms at pressures below 0.3 torr in the positive columns of dc discharges.[86-88] Kazantsev *et al.*[89] observed a difference between the orientations of the axes of optical and electronic alignment in the positive column of a dc discharge. On the basis of this difference they obtained experimental proof of an "electronic" mechanism for alignment in a plasma. The basic thrust of the laboratory experiments is to identify the mechanisms for self-alignment and to determine the atomic constants. When the physical causes of this phenomenon are known, it can be exploited for the diagnostics of low-temperature plasmas.

6. EXPERIMENTAL PROCEDURE FOR STUDYING THE INTERFERENCE OF STATES IN A LOW-TEMPERATURE PLASMA

An experimental method for studying self-alignment in the laboratory is based on the Hanle effect. An external magnetic field is applied to the part of the discharge plasma under study, and the polarization of the radiation is measured for various strengths of this external field. The resulting curve of "alignment signal" carries information about the nature of the anisotropy of the excitation, as in the astrophysical case, and it is determined by the particular characteristics of the excited level, its lifetime, and the collision cross sections.

Figure 7 shows a typical experimental arrangement for studying alignment in a discharge plasma. One studies the radiation from the plasma of the positive column of a dc gas discharge sustained in a tube with an inside diameter of the order of 1–20 mm and a length of 20–50 cm at inert gas pressures of 10^{-3}–10 torr. Some experiments have used a hollow cathode[90] and electrodeless rf discharge tubes of spherical shape 2–3 cm in diameter.[91] The source of radiation is connected to a vacuum-producing apparatus, so that measurements can be carried out at various gas pressures, measured with a McLeod gauge. The discharge is excited either by a high-voltage dc power supply or a high-frequency oscillator. The source is placed at the center of two Helmholtz coils, which create a uniform and controllable magnetic field. One pair of coils is used to produce the scanning magnetic field, while the other, coaxial with the first, is used to produce the bias field required to record the complete contour of the Hanle-effect signal. The characteristics of the coils are determined in the case of precise measurements by a magnetic-resonance method involving optically pumped vapor. The radiation from a certain part of the source is focused onto the entrance slit of a monochromator with a diffraction grating.

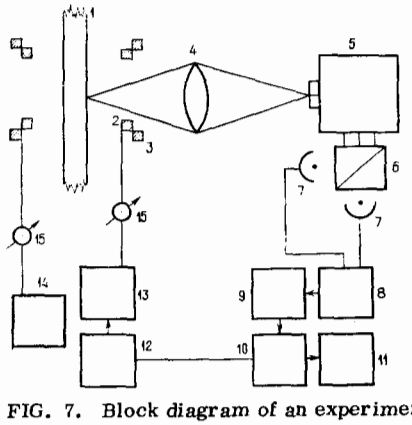

FIG. 7. Block diagram of an experimental apparatus for studying the self-alignment of excited atoms in a gas-discharge plasma. 1—Discharge tube; 2, 3—Helmholtz coils for producing a magnetic field; 4—projection lens; 5—monochromator; 6—interference polarizer; 7—photomultipliers; 8—differential amplifier; 9—analog-to-digital converter; 10—control unit; 1—pulse-height analyzer; 12—master oscillator; 13—current amplifier; 14—dc power supply; 15—instruments for measuring the current in the Helmholtz coils.

The magnetic field is directed parallel to the observation direction. Radiation linearly polarized in two orthogonal projections is singled out. When the signals in these polarizations are subtracted, the interference components are added, while the constant background is subtracted, thereby increasing the dynamic range of the measurement apparatus. With this in mind an interference polarizer is placed at the exit slit of the monochromator; it divides the radiation being investigated into two beams with mutually orthogonal polarizations. The radiation is detected with two photomultipliers, whose output signals are fed to a differential amplifier. The output signal from the differential amplifier is fed to an amplitude-to-frequency convertor, whose output pulses are fed to a pulse-height analyzer operated under conditions of slow time measurements.[92] The various channels of the analyzer are switched in synchronization with the changes in the magnetic field in the Helmholtz coils.

For this observation arrangement it is a simple matter to derive from Eqs. (12)–(16) an expression for the macroscopic-alignment signal. We assume that the alignment of the state being investigated results from an anisotropic optical excitation in a plasma. In the simplest case this process is described by an interaction of the ensemble of atoms with three weak fluxes of resonance radiation, of equal intensity, which are incident on the outer parts of the plasma and directed along the symmetry axes of the apparatus. For a cylindrical discharge tube, these fluxes are an axial flux of intensity I_1, a radial flux I_3, and a tangential flux I_2 satisfying $I_1 > I_3 > I_2$. The symmetry axes of the apparatus in which the discharge occurs determine the principal axes of the alignment tensor $\rho_q^{(2)}$, so that if the magnetic field is directed along one of the axes, and along the radius in our experimental apparatus, the alignment signal S is described by

$$S = (-1)^{J_0+J_2} A \sqrt{\frac{2J_1+1}{2J_2+1}} |(J_2 \| d \| J_1)|^2 |(J_1 \| d \| J_0)|^2 \times \begin{Bmatrix} 1 & 1 & 2 \\ J_1 & J_1 & J_0 \end{Bmatrix} \begin{Bmatrix} 1 & 1 & 2 \\ J_1 & J_1 & J_2 \end{Bmatrix} (I_1 \quad I_3) \quad \Gamma_2 + \omega^2 \cdot \tag{22}$$

Here A is a proportionality constant.

Expression (22) is written for the case in which the optical excitation occurs at the $J_0 \to J_1$ transition while the self-alignment signal corresponds to the $J_1 \to J_2$ transition.

Figure 8 shows a typical experimental alignment signal. The shape of this signal is described by Lorentzian curve (22), and the width is determined by the alignment relaxation constant Γ_2. As mentioned earlier, Γ_2 in a low-pressure gas-discharge plasma is determined by the radiative lifetime of the state of interest and by the interactions in the ensemble of atoms, including depolarizing collisions and radiation capture. Using the results of Refs. 93 and 94, we can write an explicit expression for Γ_2 under these assumptions:

$$\Gamma_2 = \Gamma_0 + \sum_{i=1}^{l} A_{1i} K_{1i} \theta_{1i} + N \langle v \sigma^{(2)} \rangle + \Gamma_{\text{coll}}^{(e)} \tag{23}$$

Here Γ_0 is the reciprocal of the radiative lifetime of the level of interest; A_{1i} is the probability for a transition from the state under study, 1, to lower-lying states i, of which there are l; N is the density of the ground-state atoms of the main gas or an admixed gas which are the perturbing particles; $\langle v \rangle$ is the average relative velocity of the colliding particles, $\sigma^{(2)}$ is the cross section for disruption of the alignment by collisions; K_{1i} is the probability for the absorption of a photon in the volume, given by the expression

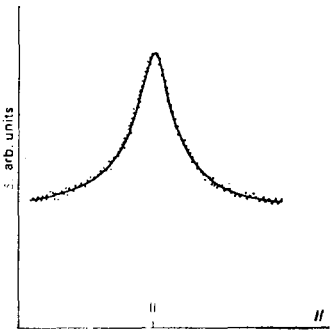

FIG. 8. Experimental self-alignment signal in the plasma of the positive column of a discharge in krypton at 7601 Å. The gas pressure is 18 mtorr, and the discharge current is 30 mA.

$$K_{1i} = \frac{1}{\sqrt{\pi}} \int_{-\infty}^{\infty} dv\, e^{-v^2} \exp(-k_{1i}^0 d\, e^{-v^2}) \tag{24}$$

in the case of a Doppler line; k_{1i}^0 is the absorption coefficient at the center of the spectral line; d is the characteristic dimension of the apparatus;

$$k_{1i}^0 = \frac{(2J_1+1)\lambda_{1i}^3 N_i A_{1i}}{(2J_i+1) 8\pi} \sqrt{\frac{m}{2\pi kT}}; \tag{25}$$

λ_{1i} is the wavelength of the $1 \to i$ transition; N_i is the density of atoms in the state i; m is the mass of the atom; k is the Boltzmann constant; T is the absolute atomic temperature; a_{1i} is a constant which depends on the total angular momenta of the levels coupled by the transition, given by

$$a_{1i} = \frac{7}{100} \times \frac{|3Y(Y-1) - 8J_1(J_1+1)|^2}{(2J_1-1)2J_1(2J_1+2)(2J_1+3)}, \quad Y = (J_1 - J_i)(J_1 - J_i + 1) + 2; \tag{26}$$

and $\Gamma_{\text{coll}}^{(e)}$ describes the relaxation of the alignment in collisions with electrons.

Determining the cross sections for depolarizing collisions involves measuring the dependence of the widths of the signal contours, $S(H)$, on the gas pressure. If the radiation capture is negligible, or if it makes a constant contribution to Γ_2 throughout the pressure range, then in the approximation of binary collisions (which is quite good for the pressure range studied, $p < 10$ torr) it varies linearly with the pressure according to (23). Figure 9 shows some representative experimental results on the widths $S(H)$ of the alignment-signal contours as functions of the pressure. Measurements of the characteristics of the alignment-signal contours yield the slope of this dependence or the pressure-induced broadening of the interference signal, $\Delta\Gamma/\Delta P$. Working from (23) we can derive a simple expression

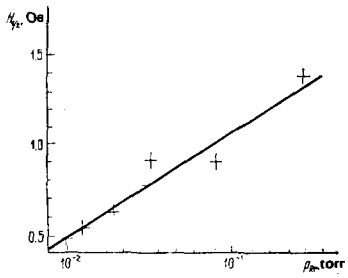

FIG. 9. Pressure dependence of the width of the self-alignment signal at the 4502 Å line of krypton (discharge current of 30 mA).

for the cross section for the collisional disruption of the alignment, $\sigma^{(2)}$:

$$\sigma^{(2)}=\frac{4.46\cdot10^{-23}\sqrt{T}}{\sqrt{\frac{1}{M_1}+\frac{1}{M_2}}}\frac{\Delta\Gamma}{\Delta P}; \qquad (27)$$

M_1 and M_2 are the atomic weights of the colliding particles (in this case, $\Delta\Gamma/\Delta P$ is expressed in megahertz per torr, and $\sigma^{(2)}$ is expressed in square centimeters).

The lifetimes of the states of interest can be found by extrapolating the widths of the alignment-signal contours to zero gas pressure. In most cases this extrapolation is linear. The nonlinearity of $\Gamma_2(P)$ at low pressures which has been observed for certain levels of inert gases stems from an effect of radiation capture or a manifestation of secondary processes.

7. RESULTS OF LABORATORY EXPERIMENTS

a) Determination of the cross sections for depolarizing collisions and lifetimes

Depolarizing collisions have been the object of many theoretical studies, which are reflected in several recent reviews and monographs.[95-100] There has been considerably less experimental work on the collisional depolarization of radiation. Tables I–V show, along with measurements taken during the observation of self-alignment in gas-discharge plasmas, the depolarization cross sections found by other experimental methods. In most studies these atomic constants have been determined by the Hanle-effect method, with a variety of methods used to excite the atomic ensemble into a coherent superposition of states. The coherent excitation in these studies was achieved using resonance optical radiation from an external source, a laser beam, collisions with a charged-particle beam, and the method described in this review: self-alignment in a discharge plasma. In some studies, information on the cross sections for the collisional disruption of alignment has been obtained by a beat method during pulsed optical and electronic excitation. Several studies have used a magnetic-resonance method with laser and electronic excitation or a saturated-absorption technique.

To study the collisional characteristics of the four levels of the electronic configuration $np^5(n+1)s$ of inert gases is a methodologically complicated problem, since the transitions to the ground state of the atom for two of these levels lie in the vacuum-ultraviolet region, while the two other levels are metastable. We have evaluated the cross sections for the depolarization of the resonant $1s_4$ level by making use of latent alignment. For the metastable $1s_5$ level, we carried out a detailed study of the collisional disruption of the orientation by atoms of the same gas and of an admixed gas. The experimental cross sections for this process are also listed in the tables.

TABLE I. Cross sections for the collisional disruption of the alignment of excited helium atoms by ground-state helium atoms (in Å^2).

State under study	Acc. Ref. 111		112, $T=293$ K	117, $T=293$ K
	$T=303$ (5) K	$T=77$ K		
3^3P	56.3 (2.1)	58.4 (3.3)		
5^3P				
3^3D			700	
4^3D			400	
3^1D				173 (20)
4^1D				268 (15)
5^1D				433 (20)
6^1D				
3^1P_1				

State under study	113, $T=292$ K	159, $T=300$ K	118, 119	77, 120, $T=340$ K
3^3P	200 (50)			
5^3P	530 (110)			
3^3D	460 (50)			
4^3D	290 (20)			
3^1D	240 (100)	240 (100)		220 (30)
4^1D	480 (50)	330 (80)	180 (10)	470 (60)
5^1D	960 (100)	600 (120)	300 (12)	850 (130)
6^1D			526 (15)	
3^1P_1				240 (20)

In compiling these tables of cross sections we noted that various definitions of the alignment-relaxation cross sections have frequently been used. In several studies (Refs. 77,78,82,86,87,102,etc.), the collisional width has been related to the cross section by $\Gamma_{coll}=\pi N\langle v\sigma^{(2)}\rangle$, which differs from (23) by the constant factor π. As a result, the depolarization cross sections found experimentally in these studies were multiplied by π before being listed in the tables.

An important factor to consider in comparing the experimental cross sections is the atomic temperature. According to (26), in order to determine a cross section from the experimental collisional broadening $\Delta\Gamma/\Delta P$ it is necessary to known the atomic temperature. In most cases, determining this characteristic is a problem in its own right, and the errors of these measurements give rise to an additional error in the cross sections. In most experiments, the atomic temperature is simply estimated roughly, with the result that systematic errors enter the results and complicate a comparison of the values obtained by different workers. For experiments in the low-temperature plasmas of the positive columns of inert gas discharges, we conclude from spectroscopic measurements[103] of the Doppler contours of spectral lines that the atomic temperature is determined by the temperature of the wall of the discharge tube.

The cross section for depolarizing collisions is known to reflect an interatomic interaction and thus to depend itself on the relative velocity of the colliding particles. This process has been studied in many theoretical papers.[99,100] For example, Faroux,[105] on the basis of the theory derived by Omont,[104] showed that in the approxi-

TABLE II. Cross sections for the depolarization of excited neon atoms in collisions with ground-state inert gas atoms (in Å^2).

State under study	Colliding atoms	Acc. Ref. 152, T= 300 K	[110] T = 85 K	[110] T = 315 K	[110] T = 840 K	[155], T = 350 K	[156], T = 340 K	[91], T = 340 K
$1s_5$	Ne—Ne	16.6 (8)						
	Ne—He	0.43 (2)						
$2p_2$	Ne—Ne		12.80 (62)	27.26 (79)	34.7 (1.7)		26.8 (1.2)	16.4 (2.5)
	Ne—He		7.28 (26)	19.74 (93)	47.5 (2.5)			
$2p_4$	Ne—Ne			92.9 (3.5)	66.3 (4.3)	66.4 (13.5)		
	Ne—He			85.0 (2.9)	70.4 (2.6)	88.8 (3.3) (He^3)		
						68.9 (3.7) (He^4)		
	Ne—Ar					(150—550)		
	Ne—Xe					(150—900)		
$2p_3$	Ne—Ne		60.9 (1.5)	53.0 (1.5)	45.9 (1.2)		53.3 (1.5)	50 (1)
	Ne—He		39.1 (1.1)	41.4 (1.1)	49.6 (1.0)			
$2p_6$	Ne—Ne		14.73 (46)	25.55 (80)	36.2 (1.7)			17.3 (1.6)
	Ne—Ne		4.68 (24)	23.41 (66)	38.9 (1.1)			
$2p_7$	Ne—Ne		60.6 (2.1)	52.0 (1.7)	43.9 (2.4)			
	Ne—He		36.9 (2.3)	37.7 (1.3)	51.7 (1.8)			
$2p_8$	Ne—Ne		81.6 (2.7)	85.2 (2.8)	72.2 (2.8)			
	Ne—He		73.7 (3.5)	79.2 (2.8)	79.9 (2.7)			
$2p_9$	Ne—Ne		111.8 (4.0)	110.7 (3.3)	98.5 (2.5)			92 (10)
	Ne—He		109.8 (3.9)	108.2 (2.9)	93.5 (2.6)			
$2p_{10}$	Ne—Ne			2.06 (29)				
	Ne—He			3.20 (32)				

State under study	Colliding atoms	Acc. Ref. 149, T=350 (20) K	[151], T = 300–350 K	[150], T = 300–350 K	[153], T=350 K	[154], T = 300 K	[86, 157, 158], T = 340 K
$1s_4$	Ne—Ne						57 (10)
$2p_2$	Ne—Ne		29 (3)				
	Ne—He		14 (2)				
$2p_4$	Ne—Ne	157 (12)		74 (5)	88 (12)	74.6 (2.1)	
	Ne—He	63 (7)		72 (5)	85	72.1 (2.1)	
$2p_5$	Ne—Ne				53 (15)		
	Ne—He				75 (15)		
$2s_4$	Ne—Ne						157 (30)
$2s_5$	Ne—Ne						167 (30)
$2d_1'$	Ne—Ne						107 (20)
$3d_3$	Ne—Ne						132 (20)
$3d_4'$	Ne—Ne						94 (28)
$3d_4$	Ne—Ne						123 (30)
$3d_5$	Ne—Ne						120 (90)
$4d_2$	Ne—Ne						470 (40)
$3s_2$	Ne—Ne			58 (5)			60 (30)
	Ne—He			24 (5)			
$5s_4$	Ne—Ne						690 (160)
$4s_4'$	Ne—Ne						660 (60)
$2s_2$	Ne—Ne			95 (20)	75 (12)	89 (10)	
	Ne—He			17 (7)	9 (3)	15.0 (1.5)	
$3p_4$	Ne—Ne				305 (50)		
	Ne—He				314 (30)		

mation of rectilinear trajectories and for an interaction potential $v(t) = -C_n(R)R^{-n}$ for the colliding atoms the cross section for the distruption of alignment depends on the relative velocity of the particles, v, as $v^{-2/n-1}$. Alternately, it varies with the temperature in proportion to $T^{-1/n-1}$ in the case of a Maxwellian distribution. For a van der Waals interaction law $[v(R) = -C_6 \cdot R^{-6}]$ the theoretical temperature dependence of the cross section is $\sigma(T) \sim T^{-1/5}$. The approach derived in these studies was used in Refs. 106–109, 83, and 84 for an impulse-approximation calculation of the cross section for the collisional realaxation of the alignment tensor of excited Ne, Ar, Kr, and Xe atoms in 2p states in interactions with inert gas atoms in the ground state. The experimental possibilities of the self-alignment method for determining collision cross sections in low-temperature plasmas are the basis for yet another research direction: measurements of the cross sections at various temperature, for various pairs of colliding atoms, to obtain information on the actual interatomic interaction. This information can be obtained by comparing the experimental values with those calculated from certain collision models. Studies of this type were carried out in Refs. 109 and 110 with reference to the 2p states of Ne and Ar atoms.

Since information about the actual atomic interaction law is usually lacking, however, it becomes a complicated matter to compare the depolarization cross sections obtained in different experiments. For a correct comparison of the constants σ^2 in Tables I–V, therefore, the cross sections are supplemented with a de-

TABLE III. Cross sections for the depolarization of excited argon atoms in collisions with ground-state inert gas atoms (in $Å^2$).

State under study	Colliding atoms	Acc. Ref. 111, $T=292$ (5) K	209, $T=300$ K	[illegible], $T=35$[illegible] (20) K	210, $T=35$[illegible] (20) K	REF. 211, $T=300$ K, accuracy of 5%	[illegible], 155, 212, $T=340$ K
$1s_5$	Ar He		6.2 (4)				
	Ar Ne		26 (2)				
	Ar Ar		100 (7)				
	Ar Xe		127				
$2p_2$	Ar He				13 (2)	8	
	Ar Ne				17 (4)	13	
	Ar Ar				66 (6)	28	114 (13)
	Ar Kr					87	
$2p_3$	Ar He				134 (9)	135	
	Ar Ne				127 (7)	132	
	Ar Ar				261 (17)	221	173 (19)
	Ar Kr				325 (20)	308	
$2p_4$	Ar He				88 (6)	91	
	Ar Ne				100 (7)	105	
	Ar Ar			182 (12)	189 (12)	145	126 (13)
	Ar Kr				249 (20)	248	
$2p_6$	Ar He				67 (5)	67	
	Ar Ne				89 (7)	92	
	Ar Ar	114 (22)		154 (19)	150 (12)	123	214 (19)
	Ar Kr				147 (11)	175	
$2p_7$	Ar He				88 (5)	112	
	Ar Ne				88 (7)	104	
	Ar Ar			185 (19)	183 (18)	145	154 (16)
	Ar Kr					239	
$2p_8$	Ar He				101 (6)	110	
	Ar Ne				122 (13)	104	
	Ar Ar				228 (15)	147	300 (30)
	Ar Kr				349 (26)	256	
$2p_9$	Ar He				128 (9)	145	
	Ar Ne				144 (12)	142	
	Ar Ar	214 (19)		229 (15)	236 (18)	197	157 (16)
	Ar Kr					278	
$3p_{10}$	Ar Ar						190 (90)
$3p_9$	Ar Ar						750 (90)
$3p_8$	Ar Ar						630 (30)
$3p_7$	Ar Ar						$1.07 (9)\cdot 10^3$
$3p_6$	Ar Ar						750 (300)
$4d_5$	Ar Ar						820 (380)
$5d_5$	Ar Ar						$2.04 (0.2)\cdot 10^3$
$6d_5$	Ar Ar						$3.9 (0.16)\cdot 10^3$

scription of the experimental conditions under which they were obtained, especially the atomic temperature.

Many studies by a variety of methods have been carried out to determine experimentally the lifetimes of excited inert gas atoms. The results obtained by the self-alignment method in a gas-discharge plasma are compared with the results found by other methods in Tables VI–XII. In most studies, the experimental lifetimes have been determined by a time analysis of the radiation for various methods for exciting the atoms: electron and ion beams, pulsed laser beams, and collisions of beam particles with targets. Extensive information on the lifetimes has been obtained by the Hanle-effect method for various versions of coherent excitation: resonance optical radiation, laser beams, and charged-particle beams. Information on the lifetimes can also be obtained from spectroscopic measurements of transition probabilities and natural line widths of levels. In several studies the lifetimes have been determined by nonlinear laser spectroscopy. Several papers have been devoted to theoretical calculations of the lifetimes of inert gas atoms; these studies have used an intermediate-coupling scheme in the single- and multiconfiguration approximations.

TABLE IV. Cross sections for the collisional depolarization of excited krypton atoms by ground-state atoms of krypton and helium-4 (in $Å^2$).

State under study	Acc. Ref. 223, $T=292$ (6) K	83, $T=300$ K	221, $T=300$ K	79, $T=340$ K
$1s_5$ (Kr – He^4)			10 (1)	
$2p_2$		406 (30)		690 (60)
$2p_3$		373 (30)		160 (60)
$2p_4$		221 (30)		
$2p_6$	449 (32)	352 (20)		940 (60)
$2p_7$		366 (30)		240 (20)
$2p_8$		387 (40)		
$2p_9$	479 (27)	358 (30)		170 (20)
$3p_8$				$1.00 (6)\cdot 10^3$
$3p_7$				$2.14 (16)\cdot 10^3$
$3p_6$				880 (160)
$3p_2$				$1.40 (13)\cdot 10^3$
$4d_4$				$1.7 (3)\cdot 10^3$
$4d_3$				690 (60)
$5d_4'$				$3.2 (3)\cdot 10^3$
$6d_4'$				$3.8 (3)\cdot 10^3$
$3s_5$				$1.26 (19)\cdot 10^3$

1) *Helium*. Table I lists the data available in the lit-

TABLE V. Cross sections for the depolarization of excited xenon atoms by ground-state inert gas atoms (in $Å^2$).

State under study	Colliding atoms	Acc. Ref. 209, $T=300$ K	84, $T=350$ K	229, $T=500$ K ($<10^3$)	230, $T=77$ K	230, $T=300$ K	224, $T=300$ K	231, $T=340$ (20) K, $\sigma^{(1)}$	231, $T=340$ (20) K, $\sigma^{(2)}$	232	80, $T=340$ K
$1s_5$	Xe—He	15 (1)									
	Xe—Ne	38 (2)									
	Xe—Ar	61 (4)									
	Xe—Xe	190 (16)			200 (59)	77 (23)	150 (40)				
					142 (92)						
$2p_3$	Xe—Xe		960 (50)								470 (280)
$2p_6$	Xe—Xe		620 (60)								
$2p_7$	Xe—Xe		570 (30)								
$2p_8$	Xe—Xe		670 (40)								
$2p_9$	Xe—He							140 (20)	230 (30)		
	Xe—Xe		340 (90)					440 (50)	810 (100)		
$2p_{10}$	Xe—He							120 (20)			
	Xe—Ar									80 (20)	
	Xe—Xe							230 (30)			
$3p_8$	Xe—Xe		$1.39 (7)\cdot 10^3$	1.7 (3)							$1.79 (28)\cdot 10^3$
$3p_6$	Xe—Xe										$2.26 (28)\cdot 10^3$
								80 (10)	90 (10)		
$3d_4$	Xe—He							170 (40)	150 (20)		
	Xe—Xe										
$5d_1'$	Xe—Xe										$2.88 (54)\cdot 10^3$
$5d_4'$	Xe—Xe										$2.51 (32)\cdot 10^3$
$6d_4'$	Xe—Xe										$3.5 (6)\cdot 10^3$

TABLE VI. Lifetimes of excited n^1D_2 states of helium atoms obtained by the self-alignment method, in comparison with other results (in ns).

3^1D_2	4^1D_2	5^1D_2	Reference
16.5 (2.0)	39.1 (2.0)	49.1 (2.0)	121
16	30	46	122
16.5 (1.0)	38 (1)		123
18 (5)	35 (4)		124
16 (2)	47 (5)	79 (6)	125
	39 (5)	63 (9)	126
12 (3)	41 (5)	49 (5)	127
16 (1)	30 (2)	46 (3)	128
	43 (5)		134
15.5 (1.5)	38 (1.5)		129
	38 (3)	66 (4)	110
	34 (4)		132
20.3 (3.0)	33.6 (3.0)	74.4 (5.0)	117
15.8 (1)	39.2 (8)	71.9 (1.8)	118
	37 (1)		133
17 (2)	33 (7)	80 (40)	77
15.3 (3)	37 (1)	69.5 (1.7)	135
		52 (6)	139
15.2 (5)	39.2 (2.3)	63.5 (5.7)	136
15.7 (1)	39.2 (1.2)		114
15.3 (3)			137
16.7 (8)	36.4 (1.2)		138

erature from measurements of the cross sections for depolarizing collisions of helium. The cross section $\sigma^{(2)}$ was determined in Ref. 111 by the Hanle-effect method for excitation by resonance optical radiation from a metastable level. A study was made of the dependence of the widths of the Hanle-effect signal contour of the 2^3P state on the helium pressure at temperatures of 303 (5) and 77 K. The resulting temperature dependence of the depolarization cross section is not the same as the theoretical dependence.[104] The difference has been attributed to repulsive forces of the interacting particles.

The cross sections for depolarizing collisions were determined in Refs. 112 and 113 by the Hanle-effect method with excitation by a particle beam. A beam of He^+ or H ions with an energy of 5–23 keV entered a helium-filled chamber. An external magnetic field perpendicular to the beam was imposed on the chamber, and a study was made of the radiation along the direction of the magnetic field. The alignment of atoms during excitation by a fast ion beam was studied in detail in Refs. 114–116. In Ref. 117 the cross sections for the depolarization of several states were determined by the Hanle method with coherent excitation of helium atoms

TABLE VII. Lifetimes of excited n^1P_1 states of the helium atom obtained by the self-alignment method in comparison with the results of other studies (in ns).

3^1P_1	4^1P_1	Reference	3^1P_1	4^1P_1	Reference
1.71		143	1.8 (1)		77
1.66 (5)		145		3.7 (4)	141
2.1		131		4.0 (4)	120
1.73 (11)		144	1.7225 (46)		140
1.8 (1)		146	1.70 (4)		136
1.72 (10)		130		4.05 (12)	

TABLE VIII. Lifetimes of the $2p^53p$ levels of the neon atom determined by the self-alignment method, in comparison with other results (in ns).

State						Reference
$2p_2$ $3p'\,[\frac{1}{2}]_1$	$2p_4$ $3p'\,[\frac{3}{2}]_2$	$2p_5$ $3p'\,[\frac{3}{2}]_1$	$2p_6$ $3p\,[\frac{3}{2}]_2$	$2p_8$ $3p\,[\frac{5}{2}]_2$	$2p_9$ $3p\,[\frac{5}{2}]_3$	
10	12.0	10.5	13.0	16.0	17.0	161
31	40	40	40	43	34	162
18.8 (3)	19.1 (3)	19.9 (4)	19.7 (2)	19.8 (2)	19.4 (6)	163
16.3 (6)	22 1	18.9 (9)	22 (1)	24.3 (8)	22.5 (9)	164
16.8 (7)						
			17 (2)			165
	14					166
18 (3)	20 (2)	20 (2)	29 (3)	25 (3)	19 (2)	167
20 (1.6)	24 (1)	23 (1)	21 (1)	25 (1)	24 (2)	168
45 (3)	30 (1)	26 (3)	26 (1)	35 (3)	20 (2)	169
	28 (1)	22 (1)	22 (1)	28 (1)		
				32 (1)		
	19.1 (6)					170
19.8 (6)	26.5 (7)	18.7 (6)	28.9 (9)	27.8 (9)	30.5 (9)	171
	26.0 (7)					
	17.0 (4)					172
20 (2)	21 (2)	22 (2)	28 (2)	23 (2)		173
	14 (6)					174
	15 (2)					175
18 (3)	21 (3)			19 (3)	26 (6)	176
19 (3)	21 (4)				26 (5)	
	23 (4)					
16.9 (8)						177
19 (1)	19 (1)	20 (2)	20 (1)	19 (1)	19 (1)	178
19 (2)	19 (2)	20 (2)	20 (2)	20 (2)		179
17 (3)	19 (4)	19 (4)	19 (4)	22 (5)		180
					23 (1,5)	181
					21.4 (9)	182
	15.9 (7)					183
	15.5 (7)					184
	24.8 (7)		25.5 (8)		23.4 (4)	185
21.0 (1)	25.0 (1)	24.0 (1)	20.0 (1)	25.5 (2)	22.5 (1)	186
17.6 (6)	19.2 (1,1)	18.6 (1.3)	18.2 (7)	19.6 (1.0)	18.7 (7)	94
16.5 (1.5)	21.5 (2.0)	19.5 (1.5)	22.0 (2.0)	22.0 (2.0)	20 (1.5)	187
				10.6 (5.1)	17.4 (3.7)	188
					21.7 (9)	189
	19.6 (2)					190
18.2 (1.1)	19 (1)	19.7 (1.2)	20.1 (1.2)	20.4 (1.2)	19.5 (1.2)	191
17.8	17.3	18.9	19.8	20.0	18.9	192
19.8 (4)	19.5 (5)	19.2 (4)	19.0 (3)	19.0 (7)	21.3 (8)	193
	18.1 (1.2)					194
19.6 (1.3)	19.8 (6)	19.5 (8)	19.1 (1.2)	17.5 (1.0)	18.0 (6)	195

TABLE IX. Lifetimes of several excited states of the neon atom determined by the self-alignment method, in comparison with other results (in ns).

$1s_2$	$1s_4$	Reference	$1s_2$	$1s_4$	Reference
	16 (8)	196	1.86	27.7	203
	20	197	1.82		204
2.7	27.4	198		22.7 (1 8)	205
2.9	20.7	198	2.5 (4)		85
	14	199	1.8	22.4	
1.52		200	1.73	23.5	206
1.45	20.8	201	1.76	23.5	
1.87 (18)	31.7 (6)	202			

State	202	207, 208		85	158
$2s_4$	9.7 (5)	11.0	8.04	8 (2)	
$2s_5$		39.4	38.8	66 (10)	
$2d_1'$		19.4	17.5 17.4	22 (1)	
$3d_3'$		27.1	24.5 26.3	25 (2)	
$3d_4'$		20.1	18.2 18.5	21 (2)	
$3d_4$		30.5	27.6 26.5	26 (2)	
$3d_5$	13.2 (6)		15.1		13.1 (1.3)
$4d_2'$			17.7		21.5 (2.0)
$3s_3'$	23 1 (1.5)		22.2		23 (2)
$5s_4'$			64.6		57 (10)
$4s_1'$			22.4		25.8 (2.0)

TABLE X. Lifetimes of several excited states of the argon atom (in ns).

State	214	215	216	217	218
$1s_2$					
$3p_{10}$		190 (3)			216 (20)
$3p_9$		141 (2)	171 (5)	63 (6)	331 (20)
$3p_8$	148 (12)	166 (5)	130 (20)	59 (6)	297 (15)
$3p_7$	190 (15)	149 (3)		121 (12)	195 (10)
$3p_6$	200 (16)	124 (3)		130 (13)	240 (15)
$4d_5$					
$4s_1'$					
$5d_5$					
$6d_5$					

State	219	220	221	87	158	222	78
$1s_2$						2.15	1.8 (4)
$3p_{10}$	140 (12)	155	114	150 (20)			
$3p_9$		124	115	185 (30)			
$3p_8$	150 (12)	134	126	135 (5)			
$3p_7$	145 (11)	126	119	130 (20)			
$3p_6$	129 (11)	110	102	140 (40)			
$4d_5$					29 (4)		
$4s_1'$					33 (5)		
$5d_5$					31 (4)		
$6d_5$					65 (10)		

TABLE XII. Lifetimes of several excited states of the xenon atom obtained by the self-alignment method, in comparison with other methods (in ns).

State	233	234	235	86
$2p_2$	39.0 (7)	34 (2)	33 (3)	38.1 (1.3)
$3p_4$	148 (11)	203 (15)	150 (10)	
$3p_3$	141 (10)		166 (10)	
$5d_1'$				
$5d_4'$				
$6d_4'$	135 (5)			
4X				

State	236	229	237	80	158
$2p_3$	30.5 (3.0)		26.5	37.4 (8)	
$3p_5$	107 (9)	169 (12)	100	190 (30)	
$3p_2$	183 (10)	163 (12)	147	200 (20)	
$5d_1'$			168	200 (30)	
$5d_4'$			143	125 (20)	
$6d_4'$				180 (25)	
4x					46 (11)

in the plasma of an rf discharge by the method described in Ref. 69. A helium-filled cell was placed inside a plane capacitor. An E-type rf discharge at a frequency of 450 MHz was excited at pressures in the range 0.1–1 torr. Alignment signals were observed in the radiation from the plasma, and their widths were studied as a function of the pressure. The use of quantum-beat spectroscopy[4] to determine the cross sections for depolarizing collisions in helium is described in Refs. 118 and 119. In these experiments, the time dependence of the amplitude of the quantum-beat signal was monitored in the case of pulsed excitation by an electron beam with an energy of 30–100 eV. Comparison of the experimental signals obtained at pressures of 0.5–400 mtorr and at magnetic fields of 1–120 Oe with the corresponding theoretical curves yielded the cross sections for depolarizing collisions of 4–6 $^1D_2$ levels. In Refs. 77 and 120, cross sections were found by the method of self-alignment in the positive column of a dc discharge in a discharge tube with an inside diameter of 6 mm, at a pressure of 0.1–0.5 torr, and at a discharge current of 50–100 mA.

The lifetimes τ of several excited levels of the helium atom which have been determined by various experimental methods are listed in Tables VI–VII. Time analysis of the radiation was used Refs. 122, 125, 126, 128, 129, 133–135, and 138 in the version of the method of delayed coincidences with electronic excitation; measurements were carried out in Refs. 130, 132, 136, 140, 140, and 141 by beam-foil and beam-gas methods. Several studies have been carried out by a method involving the interference of states in the cases of electron-impact excitation[121,123,127] and excitation by ion beams,[113,114,131,137] by the beam-foil and beam-gas methods,[139,146] and in the case of optical excitation of metastable 2^1S_0 atoms in a beam.[144] The method of self-alignment in the plasma of a positive column of a discharge was used in Refs. 77 and 120 and in the plasma of an rf discharge in Ref. 117. In a comparison of the lifetimes of the 3,4 $^1P_1$ levels it is important to note that these states are coupled by an allowed dipole transition from the ground state of the atom. Most of the experiments, therefore, involve capture of resonance radiation, which is responsible for the large scatter in the data obtained by the method of time analysis of the radiation. In Refs. 77 and 120, measurements were carried out in a pressure range in which there was total capture of resonance radiation. A corresponding theoretical study of the relaxation of the polarization moments during radiation capture was carried out in Refs. 9 and 147. In Refs. 77 and 120, the radiative lifetimes of the 3,4 $^1P_1$ levels were determined from the measured widths of the alignment signals by using the calculated results of Ref. 148. The table for these levels lists the results of the most reliable measurements made in beam experiments, in which case radiation capture is negligible.

TABLE XI. Lifetimes of excited states of the krypton atom found by the self-alignment method, in comparison with other methods (in ns).

State	225	226	227	223	83	228	79	158
$2p_9$	27	44 (3)		28 (2)	38 (3)	25.9	24 (2)	
$2p_7$		34 (2)			32 (2)	29.7	35 (1)	
$2p_6$		23 (2)		30 (2)	35 (3)	26.3	39 (3)	
$2p_3$		34 (2)			40 (4)	28.6	27 (1)	
$2p_2$		26 (2)			33 (2)	26.9	30 (4)	
$3p_8$		173 (2)	199 (4)			117	142 (7)	
$3p_7$		181 (9)	186 (6)			109	135 (5)	
$3p_6$		173 (9)	198 (4)			99.7	120 (17)	
$3p_2$			127 (2)			105	132 (7)	
$4d_4$						467	210 (40)	
$4d_3$						310	125 (8)	
$5d_4'$							220 (20)	
$6d_4'$		227 (10)					177 (20)	
$3s_5$						89.4	63 (4)	
$4d_5$								37 (10)
$3s_1'$								21 (7)

2) *Neon.* Several experimental studies have been carried out to determine the cross sections for depolarizing collisions of excited levels of neon (see Table II). Several studies in this direction have been carried out by the Hanle-effect method with a Ne-He laser.[3] The linearly polarized laser beam introduces coherence in the upper and lower levels of the lasing transition, so that the spontaneous radiation from neon at the wavelengths corresponding to transitions from these levels turns out to be polarized. An external magnetic field

imposed on the cell filled with neon or a Ne–He mixture inside a resonator disrupts the coherence of these states, and the Hanle effect is observed in the radiation recorded through the side wall of the cell. The cross sections for depolarizing collisions of the "generating" levels of neon are determined by measuring the width of the interference-signal contour as a function of the pressure of the same gas or an admixed gas. Several studies have been carried out by this method in laboratories in the USSR and abroad.[149-151,153] In Refs. 150 and 151, the cross sections listed in Table II were obtained over the temperature range 300–350 K; in Ref. 149, the temperature of the perturbing particles was 350 (20) K, and that of the excited atoms was 470 (50) K. In Ref. 153, results were obtained at 360 K. In Ref. 152, the cross sections for depolarizing collisions of the $^3P_2$ metastable level of neon were determined by an optical-orientation technique in a study of the width of the magnetic-resonance line as a function of the pressure of neon and helium at 300 K.

An extensive series of measurements of the collision cross sections in neon has been carried out by the method of self-alignment in plasmas. Collisional depolarization has been studied in greatest detail for the $2p^53p$ levels of neon.[71,81,94,106,110] The cross sections for the 2p levels of neon in collisions with neon and helium in the ground state have been measured at various temperatures; in addition, these cross sections were derived theoretically in Ref. 106 in the impulse approximation under the assumption of a dipole-dipole interatomic interaction. An analytic expression for the cross section for the collisional disruption of the alignment of these states was extracted from the results of Refs. 93 and 104, and a $T^{-1/5}$ temperature dependence was reported for the cross section. The ratio of the cross sections for depolarization by neon and helium was found to be 2.05. The experimental ratio of the cross sections for the depolarization of 2p levels by ground-state neon and helium atoms turned out to be close to the value of 1.03 (Ref. 106). This ratio was attributed to a manifestation of short-range repulsive forces in the interaction of the colliding particles. A study of the temperature dependence of the cross sections for depolarizing collisions over a broad temperature range[81,110] revealed several features which did not conform to the collision model adopted. For several of the levels, the cross section was a weak function of the temperature, in contradiction of the theory; the discrepancy was attributed to a deviation of the actual trajectories of the colliding particles from rectilinear. An increase in the cross section with increasing temperature was detected for the $2p_2$ and $2p_6$ levels. This result cannot be obtained within the framework of the adiabatic approximation. This tendency in the temperature dependence of the cross sections might be expected if inelastic processes were important in the measured cross sections, i.e., if a collisional transfer of excitation were occurring. The collisional transfer seems to be most apparent for the 2p states of neon. As a result, the collisional relaxation of the alignment of the neon 2p states is caused by two mechanisms: adiabatic collisions and inelastic collisions involving a transfer of excitation between 2p levels. The inelastic collisions become more important with increasing temperature. The cross sections for collisions which disrupt the alignment of the $2p_2$ and $2p_6$ levels, which are observed to increase with increasing temperature, and thus determined primarily by inelastic processes and are the cross sections for collisional transfer of excitation.

Yabuzaki and Manabe[155] used a double-resonance method[160] with a helium-neon laser to determine the cross sections for the collisional disruption of the alignment of the $2p_4$ levels of He^3, He^4, Ar, and Kr atoms. The cross sections for depolarizing collisions of $2p_4$ and $3s_2$ levels were determined at 300 K in Ref. 154. The quantum-beat method[4] was used in Ref. 156 to determine the cross sections for the neon $2p_5$ and $2p_4$ levels. These experiments involved pulsed laser excitation from $1s_3$ metastable levels, which were excited in a weak rf discharge. The beat signal amplitude was found to depend on the neon pressure in the range 0.1–7 torr at 340 K; the cross section for the collisional relaxation of the alignment was determined from these measurements. In Ref. 91 the cross sections for 2p levels were determined by the Hanle-effect method in the plasma of an electrodeless rf discharge in spherical spectral tubes. Measurements have been made for highly excited states in the positive column of dc gas discharges.[86,158] The cross section for depolarization of the resonance $1s_4$ level of neon was found in Ref. 157 in a study of latent alignment. The characteristics of the collisional relaxation of the alignment of the neon $1s_4$ level were found in this case from the pressure-induced broadening of the latent-alignment signal for the transition from the $2p_5$ level. The atomic temperature corresponding to the experimental conditions of Refs. 86, 91, 157, and 158 was 340–350 K.

The results of the measurements of the lifetimes of the excited neon atoms are listed in Tables VIII and IX. Table VIII gives data on the levels of the $2p^53p$ configuration. Several studies have been carried out by spectroscopic methods,[161,178,162,167,173,179,180,191] primarily by the method of spectral-line intensities. These studies have yielded experimental values for the absolute transition probabilities, and lifetimes were calculated from these probabilities. Several experiments have been carried out by direct methods involving a time analysis of the radiation accompanying pulsed excitation. The delayed-coincidence method,[163,164,168,169,182,189,202] the beam-foil method method,[176,187] and the beam-gas method[171,185] have been used here. The factor which primarily determines the accuracy of the lifetime measurements here is the excitation of the level of interest by secondary processes, primarily cascade transitions, which usually cannot be avoided. Apparently an exceptional case was Ref. 163, where measurements were taken at a fixed electron energy which exceeded the level excitation threshold by no more than 0.1–0.2 eV, and other exceptional cases were Refs. 190 and 193, where a complex beam-foil method with selective laser excitation was used. Several studies have been carried out by the method of the interference of atomic states with laser excitation[166,170,172,174,177,184] and in gas-discharge plasmas.[94] A detailed analysis of the influence

of cascade effects and of radiation capture was carried out in Ref. 94, where the systematic errors caused in the measurements by these factors were estimated experimentally. The Hanle-effect technique was used in Ref. 195 with electron-excitation. Gruzdev and Loginov[192] have derived the lifetimes for 2p levels theoretically with allowance for superposition of configurations. Table IX lists the lifetimes of the first few resonance levels and of several highly excited levels. Spectroscopic methods were used in Refs. 196, 197, 200, 201, and 204 to measure oscillator strengths and natural line widths; the delayed-coincidence method was used in the vacuum-ultraviolet region in Ref. 202. In Refs. 85, 86, 158, and 205 measurements were made by the method of self-alignment in a plasma: Latent-alignment signals were used to determine $\tau(1s_2, 1s_4)$. These constants have been derived theoretically[206-208] in the one- and multiconfiguration approximations.

3) *Argon.* Table III lists data on the cross sections for the disruption of alignment in collisions of excited argon atoms with ground-state inert gas atoms. In Ref. 111 the Hanle-effect method was used with stepped optical excitation to find the cross sections for the $2p_6$ and $2p_9$ levels at 292 (5) K. The method of optical orientation in a gas discharge was used in Ref. 209 to determine the cross sections for the depolarization of a metastable argon atom in the $1s_5$ state in collisions with ground-state inert gas atoms. These measurements were taken at room temperature. For most of the levels of the $3p^54p$ configuration of argon the cross sections for depolarization by atoms of the same gas and of admixed gases have been determined by the method of self-alignment in the plasma of an rf discharge at $T = 380$ (20) K (Refs. 82 and 210). In the case of pure argon the pressure range 0.2–1.2 torr was studied; for the case of admixtures, the ranges 0–1.2 torr (He, Ne) and 0–0.5 torr (Kr) have been studied. Parallel calculations by the model described in Ref. 106 showed that the van der Waals interaction potential gives a good description of the depolarization of 2p argon atoms in collisions with heavy atoms (Kr). In the case of light perturbing particles (He), a van der Waals simulation of the interaction leads to a discrepancey between the experimental and calculated cross sections. The nature of the interaction is more complicated in this case: Repulsive forces are manifested at short range.

The collisional relaxation of the alignment of 2p states in argon was studied in more detail in Ref. 211 by the Hanle-effect method with alignment by an external tunable dye laser. A study of the temperature dependence of the cross sections for the depolarization of this group of levels over the range 300–700 K (Ref. 212), carried out by the same method, also revealed that for heavy perturbing particles (Kr and Xe) the van der Waals interaction gives a good description of the collisional relaxation of alignment. For light perturbing atoms (He, Ne), the experimental results suggest repulsive forces in the interaction of the colliding atoms. The measurements of Refs. 87, 158, and 213 were carried out by the method of self-alignment of atoms in the plasma of the positive column of a dc discharge at pressures of 0.2–3 torr for the 2p states and at lower pressures for highly excited levels. The temperature was maintained at about 340 K.

Table VIII lists the lifetimes of the excited argon atoms. These values refer only to highly excited states and to the resonant $^1P_1$ level. Measurements of the lifetimes of the $3p^54p$ levels by the method of self-alignment in a plasma are complicated by the strong influence of the cascade transfer of alignment and radiation capture. The dealyed-coincidence method has been used in most experiments[214,215,217,222] to determine the lifetimes. These constants have been measured by the phase-shift, intensity-decay method[219] and the rf-deviation methods,[218] which is a modification of the delayed-coincidence method. It can be seen that the results of Ref. 218 overestimate τ, implying that some systematic errors have been missed. The Hanle-effect method was used in Ref. 216 with electron excitation. In Refs. 78, 87, and 158 the lifetimes have been determined by the method of self-alignment in the plasma of the positive column of a dc discharge. The lifetimes derived theoretically for these levels in an intermediate-coupling scheme through the use of the one- and multiconfiguration approximations and also in the jl-coupling scheme are reported in Refs. 220 and 221.

4) *Krypton.* Table IV lists data on the cross sections for depolarizing collisions for krypton. The cross sections for the $2p_6$ and $2p_9$ levels were found in Ref. 223 by the Hanle-effect method with optical excitation from metastable levels [$T = 292$ (6) K]. The collisional characteristics of the 2p levels of krypton were studied in Ref. 83 by the method of self-alignment in the plasma of an rf discharge at pressures 0.3–1 torr and at a power level of 20–60 W of the rf oscillator ($T = 300$ K). The cross sections for depolarizing collisions of the metastable $1s_5$ level in collisions with ground-state He^4 atoms were determined by the method of optical orientation at pressures 1–30 mtorr and at room temperature.[224] The cross sections for the disruption of the alignment of deep and highly excited states were measured by the method of self-alignment in the plasma of the positive column of a dc discharge in Ref. 79. The pressure range for the 2p states was 5–300 mtorr, and that for the highly excited states was 5–50 mtorr; the temperature was about 340 K.

Table IX lists the lifetimes of several excited levels of krypton. A reabsorption method was used in Ref. 225 to determine the absolute oscillator strength of the 8112 Å line, and the result was used to calculate the lifetime. A delayed-coincidence method was used in Refs. 226 and 227; in Ref. 223, the lifetimes of the $2p_6$ and $2p_9$ levels were measured by the Hanle-effect method in a discharge with external optical excitation. The results of Refs. 79, 83, and 158 were found by the method of self-alignment in a plasma; the experiments of Ref. 83 were carried out in an rf discharge in natural mixture of krypton isotopes, while the measurements of Refs. 79 and 158 were carried out in a dc discharge in the pure isotope Kr^{86}. These constants have been derived theoretically in the one- and multiconfiguration approximations[228] (the results corresponding to the mul-

ticonfiguration approximation are listed in the table).

5) *Xenon.* Table V gives the results found for the cross sections for depolarizing collisions of excited xenon atoms. The cross sections for the collisional disorientation of the metastable $1s_5$ level have been found in several studies[209, 224, 230] by the method of optical orientation in a discharge. A magnetic resonance was studied in Ref. 230 through a pulsed modulation of an rf field in the plasma of an E-type rf discharge in Xe^{129} at pressures in the range 10^{-4}–15 mtorr, at room temperature and liquid-nitrogen temperature. Corresponding measurements were taken in Ref. 224 at room temperature over the pressure range 1–30 mtorr in a natural mixture of xenon isotopes; the temperature in Ref. 209 was also room temperature. The discrepancies in the measured cross sections can be attributed to errors in the determination of the pressure.

For the 2p levels the cross sections for the disruption of alignment were found in Ref. 84 by the method of self-alignment in an rf discharge over the pressure range $2\cdot10^{-2}$–$5\cdot10^{-1}$ torr at 350 K. In Ref. 229, the cross sections for the collisional disruption of alignment were found by a magnetic-resonance method with electron excitation. The atomic temperature in a cell with an electron beam was estimated from measurements of the temperatures of the oxide cathode and of the collector of the electron gun; this temperature was taken to be 500 K. The pressure range studied was $4\cdot10^{-3}$–10^{-1} torr.

The method of alignment with laser excitation[231] has been used to determine the cross sections for the disruption of the alignment of the $2p_9$ and $3d_4$ levels of xenon in collisions with ground-state helium and xenon atoms. The atomic temperature was determined from the temperature of the cell wall and found to be 340 (20) K. The cross section for the collisional disruption of the alignment of the $2p_{10}$ state of xenon by ground-state argon atoms was found in Ref. 232 by the method of laser saturation spectroscopy. Cross-section measurements by the method of self-alignment in the positive column of a dc discharge[80] over the pressure range 2–50 mtorr, over the discharge-current range 20–100 mA, at 340 K revealed this characteristic for several highly excited states.

The lifetimes of excited xenon atoms are listed in Table XII. A delayed-coincidence method with electron-beam excitation was used in Refs. 233–236; the energy of the electrons exceeded the threshold for the excitation of the levels under study. The magnetic-resonance method with electron excitation was used in Ref. 229 over the pressure range 4–100 mtorr. The method of self-alignment in the plasma of an rf discharge was used in Ref. 84 to determine the lifetimes of the 2p levels, and the method of self-alignment in the plasma of the positive column of a discharge was used in Refs. 80 and 158 for several highly excited levels. These atomic constants were calculated in Ref. 237 from the intermediate-coupling model in the one- and multiconfiguration approximations.

That the method of self-alignment in a gas-discharge plasma can be used to determine the constants of various atoms and molecules has been demonstrated in a number of studies, in which lifetimes and collision cross sections have been measured for the excited levels of Hg I (Ref. 238), Cu I (Ref. 239), and Cd I (Ref. 240) and also for rotational levels of the $3d^1\Pi_g$ state of hydrogen.[241]

b) Applications of self-alignment in the diagnostics of low-temperature plasmas

The self-alignment of atoms in the plasma of a gas discharge results from the particular nature of the excitation processes. Consequently, by studying the self-alignment of excited particles we are studying these processes. Effects of this type have been observed in highly excited states of inert gas atoms in the plasma of a positive column of a dc discharge in several experiments[86–88] and have been attributed to an anisotropy of the electron-impact excitation. This mechanism for self-alignment was demonstrated experimentally in Ref. 89. According to the results of that study, the self-alignment of highly excited states results from an anisotropy of the electron velocity distribution $f(\mathrm{v})$ in a plasma at low pressures. If the problem is axisymmetric, the distribution function $f(\mathrm{v})$ in velocity space can be expanded in Legendre polynomials[251] $P_\varkappa(\cos\theta)$:

$$f(\mathrm{v}) = \sum_{\varkappa=0}^{\infty} P_\varkappa(\cos\theta)\, f^{(\varkappa)}(v); \qquad (28)$$

here θ is the angle between the velocity and the symmetry axis, and $f^{(\varkappa)}(v)$ are the multipole moments of the distribution function.

The multipole moments of the electron velocity distribution characterize the deviation from an isotropic electron distribution. The appearance of polarization moments in an ensemble in the course of electronic excitation of atoms in a gas-discharge plasma is thus related to the existence of multipole moments of the distribution function. The alignment tensor $\rho^{(2)}$ is determined by the quadrupole moment $f^{(2)}(v)$ (Ref. 252).

The possibilities of the method of self-alignment in a plasma for diagnostics were illustrated in Refs. 89, 242, and 243, where the Hanle effect in the positive column of a discharge was used to refine the nature of the motion of the fast electrons. The self-alignment of several highly excited levels of inert gas atoms was observed at low pressures, at which the electron mean free path was of the order of the diameter of the discharge tube. A theoretical description of a gas-discharge plasma corresponding to these conditions was derived in Refs. 244 and 245. This theory incorporates a radial inhomogeneity of the plasma, a transverse electric field, and the escape of fast electrons to the wall of the discharge tube. The electron gas in this approach is treated as if it were in a potential box with a height much greater than the electron energy. In the approximation of an absolutely black wall (the approximation adopted in this theory), the fastest electrons, at the tail of the Maxwellian distribution and with an energy exceeding the potential jump at the wall, can escape from the discharge plasma and be lost at the wall. Experimental confirmation of this model came from

measurements of the distribution function in the energy and the intensity of spectral lines along the radius of a discharge tube.[246-250] The total number of fast electrons with an energy sufficient to reach the wall of the discharge tube is small; the velocities of these electrons form a so-called loss cone which is oriented along the radius. The condition for the escape of an electron to the wall is

$$\frac{mv_\perp^2}{2} \geqslant eV, \qquad (29)$$

where m and e are the electron mass and charge, V is the potential jump at the wall, and $v_\perp$ is the projection of the velocity onto a plane perpendicular to the tube axis.

Condition (29) defines the loss cone. The existence of a loss cone means that there is an anisotropy of the fast electrons in the plasma in velocity space. Since the atoms and ions in a low-pressure discharge are excited by electron impact, the alignment axis must be related to the direction of the loss-cone axis. The orientation of the loss cone in velocity space is determined by the potential jump at the wall [see (29)] and, in addition, by the static axial electric field, which rotates the cone axis through a small angle with respect to the plane of the cross section of the discharge tube. The alignment axis must therefore be tilted at some angle with respect to the axis of the discharge tube, and the tilt angle is determined by the relative strengths of the axial and radial electric fields in the positive column of the discharge (Fig. 10).

In the experiments described in Ref. 89 the measured signal was the difference between the intensities of light beams with polarizations parallel and perpendicular to the axes of the discharge tube plotted as a function of the external magnetic field, oriented along the observation direction. The shape of the self-alignment signal is determined by the following expression, where the inclination of the alignment axis with respect to the symmetry axes of the discharge tube is taken into account:

$$S = \frac{A'}{\Gamma}\left(\cos 2\beta \frac{1}{1+x^2} - \sin 2\beta \frac{x}{1+x^2}\right); \qquad (30)$$

where A' is a proportionality constant, β is the inclination of the alignment axis, found from Fig. 10, and all the other notation is analogous to that used in Eq. (4).

It can be seen from (30) that the signal consists of Lorentzian and dispersive components, whose relative magnitudes are determined by the angle β. This angle is related to the ratio of the axial (E_a) and radial ($\bar{E}_r$) components of the electric field in the plasma, $E_a/\bar{E}_r$. If the discharge current is reversed without changing the the observation arrangement, then the alignment axis will go from position OO' to CC' (Fig. 10), and the angle will change to $-\beta$. As a result, the sign of the dispersive increment in the resultant signal must change. A corresponding change in the sign of the dispersive component must occur when we go to the opposite edge of the image of the discharge tube.

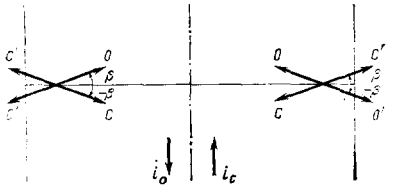

FIG. 10. Positions of the self-alignment axes near the wall in the plasma of the positive column of a gas discharge depending on the direction of the discharge current. The OO' axis corresponds to the current i_o, while CC' corresponds to i_c.

An anisotropy in the motion of fast electrons has been observed in a study of interference effects in highly excited levels of inert gas atoms.[89,243] Alignment signals have been recorded for the lines 4300 Å $\left(4s\left[\frac{3}{2}\right]_1^0 - 5p\left[\frac{5}{2}\right]_2\right)$ Ar I and 6456 Å $\left(5p\left[\frac{5}{2}\right]_3 - 6d\left[\frac{7}{2}\right]_4^0\right)$ Kr I at a pressure of 15 mtorr and, as a control, for the line 6266 Å $\left(3s'\left[\frac{1}{2}\right]_0^0 - p'\left[\frac{3}{2}\right]_1\right)$ Ne I at a pressure of 0.8 torr. Computer analysis of the signal contours revealed that in the first two of these cases there was a significant dispersive increment with a magnitude of about 5% of the amplitude of the Lorentzian component of the resultant signal. When the current was reversed, the dispersive component changed sign, in accordance with (30). The same thing happened when, for a given discharge current, the interference signals were measured from regions in the discharge tube lying near the wall and opposite each other.

In summary, these observations not only demonstrated the role played by the anisotropy of the electron pressure in forming the self-alignment of highly excited levels but also refined the orientation of the loss cone in velocity space characterizing this anisotropy.

8. CONCLUSION

Self-alignment is a universal property of light sources which leads to a partial linear polarization of their spontaneous radiation. It results from the nonequilibrium nature of the populations of particles in terms of angular-momentum projections and from an anisotropy of internal excitation processes. Self-alignment is seen under astrophysical and laboratory conditions. Astrophysical observations of this phenomenon have been made in the optical radiation from the outer part of the solar atmosphere and underlie a method for measuring weak local magnetic fields. In the laboratory, self-alignment has been observed in a low-temperature gas-discharge plasma. It has been found possible to work from the experimental results to explain the physics of self-alignment in a plasma. The reasons for the alignment are the anisotropy of the resonance photoexcitation of particles in the discharge and the anisotropy of the electron velocity distribution. Self-alignment opens up some new opportunities for the diagnostics of low-temperature plasmas and may also find use in spectroscopy as a method for measuring atomic constants. In this review we have described the physics of the phenomenon and its manifestations in astrophysical and

laboratory situations. In addition, we have summarized the results obtained by this method in laboratory measurements of atomic constants: the lifetimes and cross sections for collisional relaxation of the alignment of excited inert gas atoms. These constants can be used in astrophysical work, in particular, in practical problems involved in the magnetometry of the solar atmosphere.

I wish to thank Ya. B. Zel'dovich, D. A. Varshalovich, V. N. Rebane, and M. P. Chaĭka.

[1]S. I. Vaĭnshteĭn, Ya. B. Zel'dovich, and A. A. Ruzmaĭkin, Turbulentnoe dinamo v astrofizike (The Turbulent Dynamo in Astrophysics), Nauka, Moscow, 1980.
[2]W. Hanle, Z. Phys. **30**, 93 (1924).
[3]M. P. Chaĭka, Interferentsiya vyrozhdennykh atomnykh sostoyaniĭ (Interference of Degenerate Atomic States), Izd-vo Leningr. un-ta, Leningrad, 1975.
[4]E. B. Aleksandrov, Usp. Fiz. Nauk **107**, 595 (1972) [Sov. Phys. Usp. **15**, 436 (1973)].
[5]A. A. Ruzmaĭkin, Astron. Zh. **53**, 550 (1976) [Sov. Astron. **20**, 311 (1976)].
[6]P. P. Feofilov, Polyarizovannaya lyuminestsentsiya atomov, molekul i kristallov (Polarized Luminescence of Atoms, Molecules, and Crystals), Fizmatgiz, Moscow, 1959.
[7]V. G. Pokazan'ev and G. V. Skrotskiĭ, Usp. Fiz. Nauk **107**, 623 (1972) [Sov. Phys. Usp. **15**, 452 (1973)].
[8]L. N. Novikov, G. V. Skrotskiĭ, and G. I. Solomakho, Usp. Fiz. Nauk **113**, 597 (1974) [Sov. Phys. Usp. **17**, 542 (1975)].
[9]J. P. Barrat, J. Phys. Radium, **20**, 541, 633, 657 (1959).
[10]J. P. Barrat, Proc. R. Soc. A**263**, 371 (1961).
[11]C. Cohen-Tannoudji, Ann. Phys. (Paris) **7**, 423 (1962).
[12]M. P. Chaĭka, Avtometriya No. 1, 104 (1979).
[13]U. Fano andG. Racah, Irreducible Tensorial Sets, Academic Press, New York, 1959.
[14]M. I. D'yakonov, Zh. Eksp. Teor. Fiz. **47**, 2213 (1964) [Sov. Phys. JETP **20**, 1484 (1965)].
[15]A. Edmonds, in: Nuclear Deformation (Russ. transl. IL, Moscow, 1958).
[16]D. A. Varshalovich, A. N. Moskalev, and V. K. Khersonskiĭ, Kvantovaya teoriya uglovogo momenta (Quantum Theory of Angular Momentum), Nauka, Leningrad, 1975.
[17]S. Sahal-Brechot *et al.*, Astron. Astrophys. **59**, 223 (1977).
[18]V. Bommier and S. Sahal-Brechot, Astron. Astrophys. **69**, 57 (1978).
[19]M. Born and E. Wolf, Principles of Optics, Pergamon, New York, 1959 (Russ. transl. Nauka, Moscow, 1970).
[20]F. D. Colegrov *et al.*, Phys. Rev. Lett. **3**, 420 (1959).
[21]L. G. Zastavenko and O. A. Khrustalev, Opt. Spektrosk. **11**, 441 (1961).
[22]P. A. Frankent, Phys. Rev. **121**, 508 (1961).
[23]D. A. Varshalovich, Usp. Fiz. Nauk **101**, 369 (1970) [Sov. Phys. Usp. **13**, 429 (1971)].
[24]D. A. Varshalovich, Pis'ma Zh. Eksp. Teor. Fiz. **4**, 180 (1966) [JETP Lett. **4**, 124 (1966)].
[25]Perkins *et al.*, Astrophys. J. **145**, 361 (1966).
[26]D. A. Varshalovich, Zh. Eksp. Teor. Fiz. **56**, 614 (1969) [Sov. Phys. JETP **29**, 337 (1969)].
[27]D. A. Varshalovich and B. V. Komberg, Astron. Zh. **48**, 1085 (1971) [Sov. Astron. **15**, 858 (1972)].
[28]F. H. Mies, Astrophys. J. **202**, 823 (1975).
[29]D. A. Varshalovich and G. F. Chorny, Icarus **43**, 385 (1980).
[30]A. Unsöld, Physics of Stellar Atmospheres (in German), Springer, Göttingen (Russ. Transl. IL, Moscow, 1949).
[31]I. S. Shklovskiĭ, Fizika solnechnoĭ korony (Physics of the Solar Corona), Fizmatgiz, Moscow, 1962.
[32]Y. Ohman, Mon. Not. R. Astron. Soc. **89**, 479 (1929).
[33]B. Lyot, C. R. Acad. Sci. **198**, 249 (1934).
[34]B. Lyot, C. R. Acad. Aci. **202**, 392 (1936).
[35]H. Zanstra, Mon. Not. R. Astron. Soc. **110**, 491 (1950).
[36]G. Thiessen, Z. Astrophys. **30**, 8 (1951).
[37]C. L. Hyder, Astrophys. J. **140**, 817 (1964).
[38]J. W. Warwick and C. L. Hyder, Astrophys. J. **141**, 1362 (1965).
[39]C. L. Hyder, Astrophys. J. **141**, 1374 (1965).
[40]G. M. Nikol'skiĭ and T. S. Khetsuriani, Astron. Zh. **46**, 1040 (1969) [Sov. Astron. **13**, 815 (1970)].
[41]J. L. Leroy, G. Ratier, and V. Bommier, Astron. Astrophys. **54**, 811 (1977).
[42]V. Bommier, Astron. Astrophys. **87**, 109 (1980).
[43]V. Bommier, in: Proceedings of the International Astronomical Union Colloquium, No. 44, Oslo, August 14–18, 1978, p. 93.
[44]V. Bommier and S. Sahal-Bechot, in: Proceedings of the International Astronomical Union Colloquium, No. 44, Oslo, August 14–18, 1978, p. 87.
[45]J. M. Heasley *et al.*, Astrophys. J. **192**, 181 (1974).
[46]V. Bommier, J. L. Leroy, and S. Sahal-Brechot, Astron. Astrophys. **100**, 231 (1981).
[47]L. L. House and L. C. Cohen, Astrophys. J. **157**, 216 (1969).
[48]J. M. Beckers, in: Solar Magnetic Fields (ed. R. Howard), D. Reidel, Dordrecht, Holland, 1970, p. 3.
[49]J. O. Stenflo, Rep. Prog. Phys. **41**, 865 (1978).
[50]C. L. Hyder, Sol. Phys. **5**, 29 (1968).
[51]F. K. Lamb, Sol. Phys. **12**, 186 (1970).
[52]V. E. Stepanov and A. B. Severnyĭ, Izv. Krym. Astrofiz. Observ. **28**, 166 (1962).
[53]E. Tanberg-Hanssen, Cited in Ref. 48, p. 192.
[54]P. Charvin, Ann. Astrophys. **28**, 877 (1965).
[55]S. I. Gopasyuk, Izv. Krym. Astrofiz. Observ. **60**, 108 (1979).
[56]L. L. House, J. Quant. Spectrosc. Radiat. Transfer **10**, 909 (1970).
[57]L. L. House, J. Quant. Spectrosc. Radiat. Transfer **10**, 1171 (1970).
[58]L. L. House, J. Quant. Spectrosc. Radiat. Transfer **11**, 367 (1971).
[59]L. L. House, Sol. Phys. **23**, 103 (1972).
[60]L. L. House, Cited in Ref. 48, p. 130.
[61]C. L. Hyder, Astrophys. J. **141**, 1382 (1965).
[62]C. L. Hyder *et al.*, Astrophys. J. **154**, 1039 (1968).
[63]S. Sahal-Brechot, Astron. Astrophys. **32**, 147 (1974).
[64]S. Sahal-Brechot, Astron. Astrophys. **36**, 355 (1974).
[65]S. Sahal-Brechot, Astrophys. J. **213**, 887 (1977).
[66]J. O. Stenflo, Astron. Astrophys. **46**, 61 (1976).
[67]J. O. Stenflo and L. Stenholm, Astron. Astrophys. **46**, 69 (1976).
[68]J. O. Stenflo, Astron. Astrophys. **66**, 241 (1978).
[69]M. Lombardi and J. C. Pebay-Peyroula, C. R. Acad. Sci. **261**, 1485 (1965).
[70]Kh. Kallas and M. Chaĭka, Opt. Spektrosk. **27**, 694 (1969).
[71]C. G. Carrington and A. Corney, Opt. Commun. **1**, 115 (1969).
[72]M. P. Chaĭka, Opt. Spektrosk. **30**, 822 (1971).
[73]M. P. Chaĭka, Opt. Spektrosk. **31**, 513 (1971).
[74]M. P. Chaĭka, Opt. Spektrosk. **31**, 670 (1971).
[75]V. I. Perel' and I. V. Rogova, Zh. Eksp. Teor. Fiz. **65**, 1012 (1973) [Sov. Phys. JETP **38**, 501 (1974)].
[76]I. V. Rogova, Opt. Spektrosk. **37**, 8 (1974).
[77]S. A. Kazantsev, A. Kisling, and M. P. Chaĭka, Opt. Spektrosk. **34**, 1227 (1973).
[78]S. A. Kazantsev, A. Kisling, and M. P. Chaĭka, Opt. Spektrosk. **36**, 1030 (1974).
[79]S. A. Kazantsev, A. G. Rys', and M. P. Chaĭka, Opt. Spektrosk. **44**, 425 (1978) [Opt. Spectrosc. (USSR) **44**, 249 (1978)].
[80]S. A. Kazantsev *et al.*, Opt. Spektrosk. **46**, 1096 (1979) [Opt. Spectrosc. (USSR) **46**, 619 (1979)].
[81]C. G. Carrington and A. Corney, J. Phys. B **4**, 849 (1971).
[82]J. P. Grandin, D. Lecleur, and J. Margerie, C. R. Acad.

Sci. **272**, B929 (1971).
[83]J. P. Lemoigne, X. Husson, and J. Margerie, Opt. Commun. **15**, 241 (1975).
[84]X. Husson and J. Margerie, Opt. Commun. **5**, 139 (1972).
[85]S. A. Kazantsev, V. P. Markov, and M. P. Chaĭka, Opt. Spektrosk. **34**, 854 (1973).
[86]S. A. Kazantsev and E. S. Polzik, Opt. Spektrosk. **41**, 1092 (1976) [Opt. Spectrosc. (USSR) **41**, 645 (1976)].
[87]S. A. Kazantsev and A. G. Rys', Opt. Spektrosk. **43**, 575 (1977) [Opt. Spectrosc. (USSR) **43**, 339 (1977)].
[88]S. A. Kazantsev, in: Summaries of Contributions of the II EGAS Conference, No. 144, Paris, 1979.
[89]S. A. Kazantsev, A. G. Rys', and M. P. Chaĭka, Opt. Spektrosk. **54**, No. 2 (1983) [Opt. Spectrosc. (USSR) **54**, No. 2 (1983)].
[90]D. Zhechev, S. A. Kazantsev, and M. P. Chaĭka, in: Materialy VII Natsional'noĭ konferentsii spektroskopii (Proceedings of the Seventh Bulgarian National Conference on Spectroscopy), 1976, p. All.
[91]V. N. Grigor'eva *et al.*, Opt. Spektrosk. **54**, No. 3 (1983) [Opt. Spectrosc. (USSR) **54**, No. 3 (1983)].
[92]E. N. Kotlikov, Vestn. Leningr. un-ta No. 10, 159 (1976).
[93]M. I. D'yakonov and V. I. Perel', Zh. Eksp. Teor. Fiz. **48**, 345 (1965) [Sov. Phys. JETP **21**, 227 (1965)].
[94]C. G. Carrington, J. Phys. B **5**, 1572 (1972).
[95]B. M. Smirnov, Atomnye stolknoveniya i élementarnye protsessy v plazme (Atomic Collisions and Elementary Processes in Plasmas), Atomizdat, Moscow, 1968.
[96]E. Roueff and H. Abgrall, J. Phys. (Paris) **38**, 1485 (1977).
[97]E. E. Nikitin and A. I. Burshteĭn, in: Gazovye lazery (Gas Lasers), Nauka, Novosibirsk, 1977, p. 7.
[98]E. L. Lewis, Phys. Rep. **58**, 1 (1980).
[99]W. E. Baylis, in: Progress in Atomic Spectroscopy (ed. W. Hanle and H. Kleinpoppen) Plenum Press, New York, 1979, p. 1227.
[100]V. M. Galitskiĭ, E. E. Nikitin, and B. M. Smirnov, Teoriya stolknoveniya atomnykh chastits (Theory of the Collisions of Atomic Particles), Nauka, Moscow, 1981.
[101]J. L. Leroy, Sol. Phys. **71**, 285 (1981).
[102]A. C. G. Mitchell and M. W. Zemansky, Resonance Radiation and Excited Atoms, Macmillan, New York, 1934 (Russ. Transl. ONTI, Moscow, 1937).
[103]Yu. M. Kagan and N. N. Khristov, Opt. Spektrosk. **26**, 886 (1969).
[104]A. Omont, J. Phys. (Paris) **26**, 26 (1965).
[105]J. P. Faroux, Thesis, Paris, 1969.
[106]C. G. Carrington and A. Corney, J. Phys. B **4**, 869 (1971).
[107]J. P. Grandin, J. Phys. **34**, 403 (1973).
[108]J. P. Grandin and X. Husson, J. Phys. **39**, 933 (1978).
[109]J. P. Grandin and X. Husson, J. Phys. **42**, 33 (1981).
[110]C. G. Carrington, A. Corney, and A. V. Durrant, J. Phys. B **5**, 1001 (1972).
[111]D. A. Landman, Phys. Rev. **173**, 33 (1968).
[112]K. Buchhaupt, Z. Naturforsch. **24a**, 1058 (1969).
[113]K. Buchhaupt, Z. Naturforsch. **27a**, 572 (1972).
[114]M. Carre *et al.*, J. Phys. **38**, 553 (1977).
[115]M. Carre and M. Lombardi, J. Phys. **38**, 571 (1977).
[116]M. Carre *et al.*, J. Phys. **42**, 235 (1981).
[117]C. W. T. Chien, Can. J. Phys. **50**, 116 (1972).
[118]S. A. Bagaev *et al.*, Opt. Spektrosk. **48**, 17 (1980) [Opt. Spectrosc. (USSR) **48**, 8 (1980)].
[119]S. A. Bagaev, N. N. Evtushenko, L. P. Kantserova, and V. B. Smirnov, in: Tezisy dokladov VIII Vsesoyuznoĭ konferentsii ÉAS (Eighth All-Union Conference on Electron–Atom Collisions), Leningrad, 1981, p. 108.
[120]S. A. Kazantsev and V. P. Markov, Opt. Spektrosk. **36**, 613 (1974).
[121]B. Decomps *et al.*, C. R. Acad. Sci. **B251**, 941 (1960).
[122]P. J. Kindlmann and W. R. Bennett, Bull. Am. Phys. Soc. **8**, 87 (1963).
[123]A. Faure *et al.*, C. R. Acad. Sci. **256**, 5088 (1963).
[124]R. G. Fowler *et al.*, Proc. Phys. Soc. London **A84**, 539 (1964).
[125]W. P. Pendleton, Jr., and R. H. Hughes, Phys. Rev. **A138**, 683 (1965).
[126]K. A. Bridgett and T. A. King, Proc. Phys. Soc. London **A92**, 75 (1967).
[127]M. Maujean and J. P. Descoubes, C. R. Acad. Sci. **B264**, 1653 (1967).
[128]A. L. Osherovich and Ya. F. Verolaĭnen, Opt. Spektrosk. **24**, 162 (1968).
[129]L. Allen *et al.*, J. Opt. Soc. Am. **59**, 842 (1969).
[130]I. Martinson *et al.*, J. Opt. Soc. Am. **60**, 352 (1970).
[131]K. Buchhaupt and W. Drtill, Z. Naturforsch. **22**, 2126 (1967).
[132]S. A. ChingBing *et al.*, Am. J. Phys. **38**, 352 (1970).
[133]J. Peresse *et al.*, C. R. Acad. Sci. **274**, B791 (1972).
[134]L. L. Nicols and W. E. Wilson, Appl. Opt. **7**, 167 (1968).
[135]A. Pochat *et al.*, J. Chem. Phys. et Phys. Chim. Biol. **70**, 936 (1973).
[136]H. H. Bukow, G. Heine, and M. Reinke, J. Phys. B **10**, 2347 (1977).
[137]G. Von Oppen, Z. Phys. **A286**, 243 (1978).
[138]G. A. Khayrallah and S. J. Smith, Phys. Rev. **A18**, 559 (1978).
[139]J. Yellin *et al.*, Phys. Lett. **30**, 417 (1973).
[140]G. Astner *et al.*, Z. Phys. **A279**, 1 (1976).
[141]I. Martinson and W. S. Bickel, Phys. Lett. **A30**, 524 (1969).
[142]D. A. Varshalovich, Zh. Eksp. Teor. Fiz. **52**, 242 (1967) [Sov. Phys. JETP **25**, 157 (1967)].
[143]A. H. Gabriel and D. W. O. Heddle, Proc. R. Soc. London **A258**, 124 (1960).
[144]J. M. Burger and A. Lurio, Phys. Rev. **A3**, 64 (1971).
[145]F. A. Korolev and V. I. Odintsov, Opt. Spektrosk. **18**, 968 (1965).
[146]M. Carre *et al.*, Phys. Rev. Lett. **27**, 1407 (1971).
[147]M. I. D'yakonov and V. I. Perel', Zh. Eksp. Teor. Fiz. **47**, 1483 (1964) [Sov. Phys. JETP **20**, 997 (1965)].
[148]M. P. Chaĭka, Opt. Spektrosk. **39**, 1015 (1975) [Opt. Spectrosc. (USSR) **39**, 582 (1975)].
[149]T. Hansch *et al.*, Z. Phys. **209**, 478 (1968).
[150]B. Decomps and M. Dumont, IEEE J. Quantum Electron. **QE-4**, 916 (1968).
[151]F. Fournier *et al.*, C. R. Acad. Sci. **B268**, 1495 (1969).
[152]L. D. Schearer, Phys. Rev. **180**, 83 (1969).
[153]N. I. Kaliteevskiĭ *et al.*, Kvant. Elektron. (Moscow) **4**, 1949 (1977) [Sov. J. Quantum Electron. **7**, 1107 (1977)].
[154]F. Grauber and G. Hermann, Z. Phys. **A289**, 21 (1978).
[155]T. Yabuzaki and T. Manabe, J. Phys. Soc. Jpn. **47**, 343 (1979).
[156]J. R. Bradenberger and B. R. Rose, Opt. Commun. **36**, 453 (1981).
[157]S. A. Kazantsev and M. P. Chaĭka, Opt. Spektrosk. **31**, 510 (1971).
[158]S. A. Kazantsev and V. I. Éĭduk, Opt. Spektrosk. **45**, 858 (1978) [Opt. Spectrosc. (USSR) **45**, 735 (1978)].
[159]M. Pinard and J. van der Linde, Can. J. Phys. **52**, 1615 (1974).
[160]G. W. Series, Phys. Soc. Rep. Prog. Phys. **22**, 280 (1959).
[161]R. Ladenburg, Rev. Mod. Phys. **5**, 243 (1933).
[162]L. R. Doherty, PhD Thesis, Michigan, 1962.
[163]W. R. Bennet and P. J. Kindlmann, Phys. Rev. **149**, 38 (1966).
[164]J. Z. Klose, Phys. Rev. **141**, 181 (1966).
[165]D. Rosenberger and J. Thum, Z. Naturforsch. **21a**, 175 (1966).
[166]Th. Hänsch and P. Toschek, Phys. Lett. **22**, 151 (1966).
[167]J. C. Irwin and R. A. Nodwell, Can. J. Phys. **44**, 1781 (1966).
[168]A. L. Osherovich and Ya. F. Verolaĭnen, Opt. Spektrosk. **22**, 329 (1967).
[169]I. Bakoshi and I. Sigeti, Opt. Spektrosk. **23**, 478 (1967).

[170]Th. Hänsch *et al.*, Z. Phys. **209**, 478 (1968).
[171]A. Denis *et al.*, C. R. Acad. Sci. **B266**, 1016 (1968).
[172]B. Decomps and M. Dumont, IEEE J. Quantum Electron. **QE-4**, 916 (1968).
[173]R. A. Nodwell *et al.*, J. Quant. Spectrosc. Radiat. Transfer **8**, 859 (1968).
[174]Kh. V. Kallas, V. N. Rebane, and M. P. Chaĭka, in: Fizika gazovykh lazerov (Physics of Gas Lasers), Izd-vo Leningr. un-ta, Leningrad, 1969, p. 94.
[175]É. I. Ivanov and M. P. Chaika, Opt. Spektrosk. **29**, 625 (1970).
[176]C. E. Assousa *et al.*, J. Opt. Soc. Am. **60**, 1311 (1970).
[177]M. Ducloy *et al.*, J. Phys. **31**, 533 (1970).
[178]J. M. Bridges and W. L. Wiese, Phys. Rev. **A2**, 285 (1970).
[179]D. R. Shofstall and D. G. Ellis, J. Opt. Soc. Am. **60**, 894 (1970).
[180]R. D. Bengtson and M. H. Miller, J. Opt. Soc. Am. **60**, 1093 (1970).
[181]C. H. Liu *et al.*, Phys. Rev. Lett. **26**, 222 (1971).
[182]J. A. Kohl *et al.*, J. Opt. Soc. Am. **61**, 1656 (1971).
[183]R. Arrathon and D. A. Sealer, Phys. Rev. **A4**, 815 (1971).
[184]G. Ts. Todorov, Candidate's Dissertation, Leningrad 1973.
[185]T. N. Lawrence and C. E. Head, Phys. Rev. **A8**, 1644 (1973).
[186]A. L. Osherovich and V. N. Ivanov, Vestn. Leningr. un-ta No. 22, 154 (1973).
[187]T. Anderson, Nucl. Instrum. Methods **110**, 35 (1973).
[188]A. Yamagishi and H. Inaba, Opt. Commun. **12**, 213 (1974).
[189]R. M. Shectman *et al.*, J. Opt. Soc. Am. **63**, 99 (1973).
[190]H. Harde and G. Guthohrlein, Phys. Rev. **A10**, 1488 (1974).
[191]S. Inatsugu and J. R. Holmes, Phys. Rev. **A11**, 26 (1975).
[192]P. F. Gruzdev and A. V. Loginov, Opt. Spektrosk. **45**, 1050 (1978) [Opt. Spectrosc. (USSR) **45**, 846 (1978)].
[193]R. S. F. Chang and D. M. Setser, J. Chem. Phys. **72**, 4099 (1980).
[194]Im. Tkhek-de, S. G. Rautian, É. G. Saprykin, and A. M. Shalagin, Opt. Spektrosk. **49**, 438 (1980) [Opt. Spectrosc. (USSR) **49**, 240 (1980)].
[195]I. P. Bogdanova, S. A. Kazantsev, and M. P. Chaĭka, Opt. Spektrosk. **54**, No. 4 (1983) [Opt. Spectrosc. (USSR) **54**, No. 4 (1983)].
[196]W. Shütz, Ann. Phys. (Leipzig) **18**, 705 (1933).
[197]A. Phelps, Phys. Rev. **100**, 1230 (1955).
[198]A. Gold and R. Knox, Phys. Rev. **113**, 834 (1959).
[199]Stats *et al.*, J. Appl. Phys. **34**, 2625 (1963).
[200]F. Korolev *et al.*, Opt. Spektrosk. **16**, 555 (1964).
[201]E. Lewis, Proc. Phys. Soc. **92**, 817 (1967).
[202]G. Lawrence and H. Liszi, Phys. Rev. **178**, 122 (1969).
[203]J. Geiger, Phys. Lett. A33, 315 (1970).
[204]J. Jongh and J. Eck, Physica (Utrecht) **51**, 104 (1971).
[205]S. A. Kazantsev *et al.*, Opt. Spektrosk. **45**, 816 (1978) [Opt. Spectrosc. (USSR) **45**, 711 (1978)].
[206]P. F. Gruzdev and A. V. Loginov, Opt. Spektrosk. **53**, 3 (1973).
[207]N. V. Afanas'eva and P. F. Gruzdev, Opt. Spektrosk. **38**, 378 (1975) [Opt. Spectrosc. (USSR) **38**, 211 (1975)].
[208]P. F. Gruzdev and A. V. Loginov, Opt. Spektrosk. **38**, 411, 1056 (1975) [Opt. Spectrosc. (USSR) **38**, 234, 611 (1975)].
[209]L. D. Schearer, Phys. Rev. **188**, 505 (1969).
[210]J. P. Grandin, J. Phys. (Paris) **34**, 403 (1973).
[211]J. P. Grandin and X. Hausson, J. Phys. (Paris) **39**, 933 (1978).
[212]J. P. Grandin and X. Husson, J. Phys. (Paris) **42**, 33 (1981).
[213]S. A. Kazantsev, Author's Abstract, Candidate's Dissertation, LGU, Leningrad, 1973.
[214]Ya. F. Verolaĭnen andA. L. Osherovich, Opt. Spektrosk. **25**, 466 (1968).
[215]J. Z. Klose, J. Opt. Soc. Am. **58**, 1509 (1968).
[216]M. Chenevier and G. Goullet, J. Phys. **30**, C1-82 (1969).
[217]Yu. I. Malakhov and V. G. Potemkin, Opt. Spektrosk. **32**, 245 (1972).
[218]P. Erman and I. Martinson, Phys. Scripta **8**, 269 (1973).
[219]A. L. Yusherovich *et al.*, Vestn. Leningr. un-ta No. 22, 7 (1974).
[220]P. F. Gruzdev and A. V. Loginov, Opt. Spektrosk. **38**, 411 (1975) [Opt. Spectrosc. (USSR) **38**, 234 (1975)].
[221]N. V. Afanas'eva and P. F. Gruzdev, Opt. Spektrosk. **38**, 794 (1975) [Opt. Spectrosc. (USSR) **38**, 450 (1975)].
[222]G. H. Lawrence, Phys. Rev. **175**, 40 (1968).
[223]D. A. Landman and R. Dobrin, Phys. Rev. **A8**, 1868 (1973).
[224]V. Lefevre Seguin and M. Leduc, J. Phys. B **10**, 2157 (1977).
[225]V. P. Malakhov, Izv. Vyssh. Uchebn. Zaved., Fiz. No. 1, 1801 (1965).
[226]A. L. Osherovich and Ya. F. Verolaĭnen, Vestn. Leningr. un-ta, No. 1, 140 (1967).
[227]A. Delgado *et al.*, Z. Phys. **257**, 9 (1972).
[228]P. F. Gruzdev and A. V. Loginov, Opt. Spektrosk. **38**, 1056 (1975) [Opt. Spectrosc. (USSR) **38**, 611 (1975)].
[229]M. Chenevier and P. A. Moskowitz, J. Phys. (Paris) **35**, 410 (1974).
[230]R. A. Zhitnikov and A. I. Okunevich, Opt. Spektrosk. **36**, 438 (1974).
[231]T. Suzuki and K. Shimoda, J. Phys. Soc. Jpn. **43**, 233 (1977).
[232]J.-L. Le Gouet and R. Vetter, J. Phys. B **13**, L147 (1980).
[233]L. Allen and D. Johes, J. Opt. Soc. Am. **59**, 842 (1969).
[234]Ya. F. Verolaĭnen and A. L. Osherovich, Opt. Spektrosk. **27**, 31 (1969).
[235]R. G. Karimov and V. M. Koimkin, Izv. Vyssh. Uchebn. Zaved., Fiz. **3**, 24 (1971).
[236]E. Jimenez *et al.*, J. Opt. Soc. Am. **64**, 1007 (1974).
[237]P. F. Gruzdev and A. V. Loginov, Opt. Spektrosk. **41**, 176 (1976) [Opt. Spectrosc. (USSR) **41**, 104 (1976)].
[238]É. A. Alipieva and E. N. Kotlikov, Opt. Spektrosk. **43**, 1000 (1977) [Opt. Spectrosc. (USSR) **43**, 592 (1977)].
[239]D. Z. Zhechev, Opt. Spektrosk. **49**, 465 (1980) [Opt. Spectrosc. (USSR) **49**, 253 (1980)].
[240]A. R. Atadzhanov, E. N. Kotlikov, and M. P. Chaĭka, Opt. Spektrosk. **50**, 817 (1981) [Opt. Spectrosc. (USSR) **50**, 447 (1981)].
[241]E. N. Kotlikov and A. P. Bryukhovetskiĭ, Opt. Spektrosk. **49**, 1105 (1980) [Opt. Spectrosc. (USSR) **49**, 603 (1980)].
[242]S. A. Kazantsev, Opt. Spektrosk. **52**, 931 (1982) [Opt. Spectrosc. (USSR) **52**, 559 (1982)].
[243]S. A. Kazantzev, A. G. Rys, and M. P. Chaĭka, in: Pro-Proceedings of the International Conference on Phenomena of Ionized Gases, Minsk, 1981, p. 419.
[244]L. D. Tsendin, Zh. Eksp. Teor. Fiz. **66**, 1638 (1974) [Sov. Phys. JETP **39**, 805 (1974)].
[245]L. D. Tsendin and Yu. B. Golubovskiĭ, Zh. Tekh. Fiz. **47**, 1839 (1977) [Sov. Phys. Tech. Phys. **22**, 1066 (1977)].
[246]V. V. Zaitsev and V. M. Milenin, Zh. Tekh. Fiz. **49**, 2521 (1979) [*sic*].
[247]N. A. Vorob'eva, V. M. Milenin, and L. D. Tsendin, Zh. Tekh. Fiz. **49**, 763 (1979) [Sov. Phys. Tech. Phys. **24**, 442 (1979)].
[248]V. V. Zaĭtsev *et al.*, Teplofiz. Vys Temp. **17**, 20 (1979).
[249]V. V. Zaĭtsev *et al.*, Teplofiz. Vys. Temp. **18**, 944 (1980).
[250]V. M. Milenin, Opt. Spektrosk. **46**, 1209 (1979) [Opt. Spectrosc. (USSR) **46**, 683 (1979)].
[251]V. L. Ginzburg and A. V. Gurevich, Usp. Fiz. Nauk **70**, 201 393 (1960) [Sov. Phys. Usp. **3**, 175 (1960)].
[252]S. A. Kazantsev, Pis'ma Zh. Eksp. Teor. Fiz. **37**, 131 (1983) [JETP Lett. **37**, 158 (1983)].

Translated by Dave Parsons